



VILNIUS UNIVERSITY
LIFE SCIENCES CENTER
Eglė Meškauskaitė

**Anatomical alterations in the contralateral brain hemisphere
in an ischemic stroke model (tMCAo)**

Master's Thesis

Neurobiology study program

Thesis supervisor

Dr. Asta Kastanauskaitė

Consultant

Dr. Paula Merino-Serrais

Thesis completed at

Cajal Cortical Circuits Laboratory, Cajal
Institute, UPM-CSIC, Madrid, Spain

Content

Abbreviations.....	3
1. Introduction.....	4
2. Literature analysis.....	6
2.1. Stroke definition and epidemiology.....	6
2.2. Symptoms and risk factors.....	7
2.3. Types of stroke.....	8
2.4. Etiology of stroke.....	8
2.5. Pathophysiology of stroke.....	9
2.6. Diagnosis and treatment of stroke.....	11
2.7. Consequences of stroke.....	13
2.8. Animal models of ischemic stroke.....	14
2.9. Brain anatomy and lateralisation.....	17
2.10. Cortical areas and subcortical structures.....	18
2.11. Cortical layers, white matter and blood supply.....	19
2.12. Types of cortical neurons.....	21
2.13. Comparison between human and mouse brain.....	21
2.14. Cortical alterations after ischemic stroke and diaschisis.....	22
3. Materials and methods.....	25
3.1. Animals and sample processing.....	25
3.2. Sample selection and Nissl staining.....	26
3.3. Estimation of brain areas and thickness.....	27
3.4. Statistical Analysis.....	29
4. Results.....	31
4.1. Alterations in total area of both hemispheres and corpus callosum.....	31
4.2. Alterations in total area of cortical areas.....	34
4.3. Alterations in total area of subcortical areas.....	37
4.4. Alterations in the thickness of cortical areas and hippocampal formation.....	40
Discussion.....	43
Conclusions and recommendations.....	46
Authors personal contribution.....	47
Acknowledgments.....	47
Funding.....	47
Santrauka.....	48
Abstract.....	49
References.....	50

Abbreviations

3R - replacement, reduction, refinement
ACA - anterior cerebral artery
ATP - adenosine triphosphate
BBB - blood brain barrier
CCA - common carotid artery
CT - computed tomography
CVA - cerebrovascular accident
DALY's - disability-adjusted life years lost
EEG-EMG - electroencephalogram-electromyogram
ET-1 - endothelin 1
GABA- gamma-aminobutyric acid
HDL - high density lipoprotein
HIF-1 - hypoxia-induced factor 1
hsCRP - high-sensitivity assay C-reactive protein
ICA - internal carotid artery
IV - intravenous
LAA - large-artery atherosclerosis
MRI - magnetic resonance imaging
mTORC1 - mechanistic target of rapamycin complex 1
NINDS - National Institute of Neurological Disorders and Stroke
NMDAR's - N-methyl-D-aspartate receptors
PBS - phosphate buffered saline
PCA - posterior cerebral artery
PFA - paraformaldehyde
ROS - reactive oxygen species
rtPA - recombinant tissue plasminogen activator
SEM - standard error of the mean
TIA - transient ischemic attack
tMCAo or MCAo - (transient) middle cerebral artery occlusion
TMS - transcranial magnetic stimulation
WHO - World Health Organisation
WMI - white matter injury
WM - white matter

1. Introduction

Stroke, commonly known as a cerebrovascular accident, is a global epidemic as it is the second leading cause of mortality and a leading cause of long-term disability worldwide. It is characterised by the sudden disruption of blood flow to the brain, resulting in neuronal injury or death. The most common type of stroke, accounting for 85% of all cases, is ischemic stroke, which is caused by a blood vessel blockage in the brain, leading to insufficient oxygen and nutrient delivery to brain cells. The severity of damage depends on the location and duration of ischemia, making it a critical focus of neurological research.

Understanding the underlying mechanisms of ischemic stroke is crucial for improving treatment strategies as they are extremely limited. The pathophysiology of stroke is complex, involving a complex cascade of events such as excitotoxicity, oxidative stress, inflammation and apoptosis which can all lead to permanent brain damage. These events are not only localised to the infarcted brain areas but also induce widespread anatomical and structural alterations in connected brain regions in a phenomenon known as diaschisis. This concept highlights that the impact of stroke extends beyond the primary lesion, affecting distant but functionally connected brain regions, hence, playing an important role in post-stroke treatment and recovery. Although the research of diaschisis is relatively recent, it has gained more attention due to the advancements in neuroimaging techniques which allow more detailed visualisation of the whole-brain connectome and facilitate the analysis of contralesional changes.

In addition to primary cortical areas such as somatosensory, motor and visual, subcortical areas including the corpus callosum, amygdaloid complex, thalamus, hypothalamus, hippocampal formation and dorsal striatum can also be affected during stroke. These structures play crucial roles in sensory processing, memory and emotional regulation which makes them vital for overall neurological function.

This master's thesis focuses on analysing the anatomical alterations in cortical and subcortical structures following ischemic stroke, using the middle cerebral artery occlusion (tMCAo) model in mice. This model is widely used due to its ability to replicate the pathophysiology of human ischemic stroke closely. By examining structural changes in total area and thickness of mentioned regions and comparing them between Sham (control) and tMCAo (experimental) groups, this study aims to provide insights into the extent and nature of post-stroke damage, contributing to better understanding of stroke pathology and potential therapeutic targets.

Main objectives:

1. To study alterations in the total area of cortical and subcortical structures on the ipsilateral to the lesion and contralateral to the lesion sides between Sham and tMCAo groups, identifying significant differences in selected brain regions (hemispheres, corpus callosum, somatosensory cortex, motor cortex, visual cortex, amygdaloid complex, thalamus, hypothalamus, hippocampal formation and dorsal striatum).
2. To study alterations in the thickness of cortical and subcortical structures on the ipsilateral to the lesion and contralateral to the lesion sides between Sham and tMCAo groups, identifying significant differences in selected brain regions (somatosensory cortex, motor cortex, visual cortex and hippocampal formation).
3. To explore the concept of diaschisis by investigating the relationship between ischemic stroke lesion and post-stroke changes in connected regions.

2. Literature analysis

2.1. Stroke definition and epidemiology

Stroke, also known as cerebrovascular accident (CVA) or "*ictus*" in Latin, is a neurological emergency that occurs when the blood flow to the brain is impaired (blocked). This leads to ischemia or **ischemic stroke**, in which case there is an insufficient oxygen and nutrient delivery to brain cells, resulting in neuronal injury or death. There is another type of stroke known as **hemorrhagic stroke** in which there is a rupture of a blood vessel causing bleeding into or around the brain tissue hence, damaging the brain tissue further. It is important to note that another vascular entity, known as transient ischemic attack (TIA), may sound like a stroke, but it is more like a "mini-stroke" which lasts less than 24 hours, produces no permanent brain damage, yet, it is a signal of impending stroke (Kleindorfer et al., 2005).

Stroke is not consistently defined in clinical practice, research and public health, yet clinically, it is defined by abrupt onset of focal neurological dysfunction caused by acute vascular injury in the brain that lasts more than 24 hours or leads to early death (Warlow et al., 2011). Due to advancements in technology, an updated definition of stroke was proposed, which states, that stroke is an acute event involving localised dysfunction of the brain, retina or spinal cord, regardless of its duration, where imaging techniques such as computed tomography (CT), magnetic resonance imaging (MRI) or autopsy reveal a corresponding area of infarction or hemorrhage consistent with the clinical symptoms (Sacco et al., 2013).

Nowadays, stroke is a major global health concern as it is a second leading cause of mortality and a leading cause of long-term disability (Feigin et al., 2022). It impacts approximately 13,7 million individuals each year and results in around 5,5 million deaths annually (Kuriakose & Xiao, 2020). In Western countries, stroke accounts for approximately 10-12% of all deaths with 12% of these fatalities occurring in individuals under the age of 65 (Bonita, 1992). In recent decades, despite the reduction in mortality rate and better stabilization after the stroke, it is considered a modern epidemic (Li et al., 2017), due to the high number of prevalent cases and disability-adjusted life years lost (DALY's). According to the World Health Organisation (WHO), DALY measures overall disease burden by combining years lost to premature death with years lived with disability due to illness or injury, not only showing how many people die, but also how many people live with long-term health issues from diseases like stroke (World Health Organization, 2024).

Stroke incidence varies significantly across Europe, with the highest rates observed in Eastern and Northern regions, including Lithuania and the city of Kaunas (Radisauskas et al., 2016). Lithuania has one of the highest rates of acute ischemic stroke and stroke-related mortality globally (Kim et al., 2020) due to inadequate management of cardiovascular risk factors (Laucevičius et al., 2020)

such as high cholesterol and hypertension. In Lithuania, the number of new stroke cases per 100,000 inhabitants was approximately 190 in 1995 and declined slightly to around 170 by 2015. During the same period, the number of stroke survivors per 100,000 remained relatively stable - about 940 in 1995 and 910 in 2015. When examining the number of deaths and DALYs per 100,000 people, a noticeable improvement is evident: stroke-related deaths dropped from around 140 to 80 and DALYs decreased from around 2300 to 1300. Despite these improvements, Lithuania still recorded one of the highest stroke mortality rates in Europe. Furthermore, projections suggest that between 2015 and 2035, stroke-related death rates in Lithuania will rise by 10% and DALYs are expected to increase by 1% (Stevens et al., 2017).

2.2. Symptoms and risk factors

Typically, stroke occurs spontaneously and is characterised by the sudden or rapidly evolving loss of function in specific body regions, resulting from dysfunction in a corresponding area of the brain, retina or spinal cord. Some common focal neurological symptoms, which help localise the stroke region and can occur in isolation or combination include: unilateral weakness, unilateral sensory loss, monocular vision loss, hemianopic visual field deficient, double vision, speech impairment, visual-spatial and perceptual disturbances, clumsiness or ataxia and vertigo (Hankey and Blacker, 2015). Less commonly, stroke can result in atypical presentations called “chameleons” that imitate other neurological conditions (Fernandes et al., 2013).

The risk factors of stroke can be divided into two main groups: non-modifiable and modifiable risk factors. The non-modifiable risk factors include age, sex, race and genetics (Boehme et al., 2017). Stroke incidence doubles after 55 years of age (Roger et al., 2012). Also, the link between sex and stroke risk varies with age as in younger individuals, women have an equal or slightly higher risk than men, while in older age groups, men tend to have slightly increased risk of stroke (Iaccarino et al., 2005). When it comes to the differences of race, black people tend to have two times higher risk of stroke compared to white people (Cruz-Flores et al., 2011). Also, genetic risk factors contribute to increased risk for both ischemic and hemorrhagic stroke through the presence of the $\epsilon 2$ and $\epsilon 4$ alleles of the APOE gene (Chauhan & Debette, 2016).

The modifiable risk factors are crucial for intervention. Hypertension is the most important, increasing risk even in non hypertensive individuals (Stansbury et al., 2005) and affecting two-thirds of people over 65 years (Chobanian et al., 2003). Diabetes mellitus doubles the risk of stroke, with 20% of diabetic deaths caused by stroke (Banerjee et al., 2012). Atrial fibrillation, which is a common type of cardiac arrhythmia, tends to triple stroke incidence over 30 years (Yiin et al., 2014).

2.3. Types of stroke

There are two primary types of stroke: **hemorrhagic** and **ischemic**. In hemorrhagic stroke, which accounts for approximately 15 % of stroke cases, there is a rupture of a blood vessel in or around the brain, which leads to intracerebral (ventricular system) or subarachnoid hemorrhage. Interestingly, in low-income countries, intracerebral hemorrhage accounts for 30% of stroke cases and its fatality rate is higher than ischemic, resulting in 2,8 million deaths and 64,5 million DALYs in 2016 (Hilkens et al., 2024). The most frequent causes include hypertension, cerebral amyloid angiopathy, anticoagulant use and vascular structural abnormalities (Rannikmäe et al., 2016).

In ischemic stroke, which accounts for approximately 85% of stroke cases, there is an occlusion of a cerebral artery due to a blood clot, embolus or systemic hypoperfusion (reduced amount of blood flow) which causes blockage of blood supply to the brain and results in cerebral infarct. In 2021, out of 11,9 million newly diagnosed stroke cases, 65,3% were ischemic, resulting in 7,3 million deaths and 160,5 million DALYs lost (GBD 2021 Stroke Risk Factor Collaborators, 2024).

2.4. Etiology of stroke

It is very important to classify the etiology of ischemic stroke as it impacts the course of the disease, treatment and recovery. Ischemic strokes can be classified according to the Trial of Org 10172 in Acute Stroke Treatment (TOAST) criteria which categorises strokes based on their underlying etiology into five subtypes: large-artery atherosclerosis (LAA), cardioembolism, small vessel occlusion (lacune), stroke of other determined etiology and stroke of undetermined etiology (Adams et al., 1993).

LAA accounts for 15-37% of ischemic stroke causes (Chaturvedi and Bhattacharya, 2014) and is characterised by clinical presentation and neuroimaging evidence indicating significant narrowing (stenosis) or complete occlusion of a major cerebral artery, such as the carotid or vertebral arteries, or one of their cortical branches, including the anterior, middle or posterior cerebral arteries (Cole, 2017). LAA can lead to stroke through two main pathophysiological mechanisms: hypoperfusion resulting from hemodynamically significant arterial stenosis or atheroembolism caused by plaque rupture or ulceration, leading to thrombus formation and subsequent embolisation to downstream cerebral vessels (Maitrias et al., 2017).

Cardioembolic strokes account for 20% of ischemic strokes and are generally associated with greater severity compared to other types of ischemic stroke (Lin et al., 1996) as they occlude large intracranial vessels, resulting in larger area of ischemia. The most common cause of it is atrial fibrillation while other causes include ventricular thrombi resulting from myocardial infarction or heart failure, structural heart abnormalities, atheroma of the aortic arch and even infections like endocarditis (Freeman & Aguilar, 2008).

Small vessel occlusion within the brain is believed to be the main cause of most small but deep lacunar infarcts (Alistair, 2000). It accounts for 20% of ischemic strokes and primarily involves smaller blood vessels in the brain such as perforating arterioles, capillaries and venules (Ter Telgte et al., 2018). This subtype is notably severe, with a recurrence rate of 20% and a five-year mortality rate of 25% (Regenhardt et al., 2018). The main causes of it can be common, such as destructive small vessel disease (lipohyalinosis) or perforating artery atherosclerosis and uncommon, such as embolism, vasculitis, infection, hypoperfusion, arterial dissection and cerebral amyloid angiopathy (Alistair, 2000).

Strokes of other determined or undetermined etiology include patients whose strokes result from rare causes such as non-atherosclerotic vascular disorders, hypercoagulable conditions and hematological conditions. In these cases, CT or MRI scans together with blood tests or arteriography help reveal more accurate causes. In undetermined cases the reason for stroke cannot be identified or it has multiple causes preventing a clear and conclusive diagnosis (Adams et al., 1993).

2.5. Pathophysiology of stroke

Understanding the pathophysiology of any disease is crucial when it comes to the treatment of it. In case of stroke, despite its significant health and socioeconomic impact, effective pharmacological treatments for ischemic stroke remain limited, therefore, it is crucial to clearly understand what events take place during the event of stroke.

When the blood supply to the brain tissue is interrupted, the region of the brain directly impacted by the stroke is referred to as the **ischemic core**, where the majority of cells experience irreversible damage before neuroprotective treatments can exert their effects. The area surrounding the ischemic core is called the **ischemic penumbra**. It is a zone of potentially salvageable tissue that often serves as the primary focus of therapeutic intervention. Moreover, a complex interplay of molecular and cellular mechanisms within these regions leads to various clinical manifestations such as hemiplegia, paraplegia, dysarthria and paresis with additional symptoms depending on specific brain areas affected by blood flow disruption.

Similar to other neurodegenerative diseases, ischemic stroke is marked by a cascade of changes within the ischemic core and penumbra, called **ischemic cascade**, which initially can lead to **infarction** (irreversible tissue damage). These processes are grouped into five pathological processes that all lead to cell death: neuroinflammation, excitotoxicity, neurochemical injury (oxidative stress) and apoptosis and autophagy (see figure 1) (Salaudeen et al., 2024).

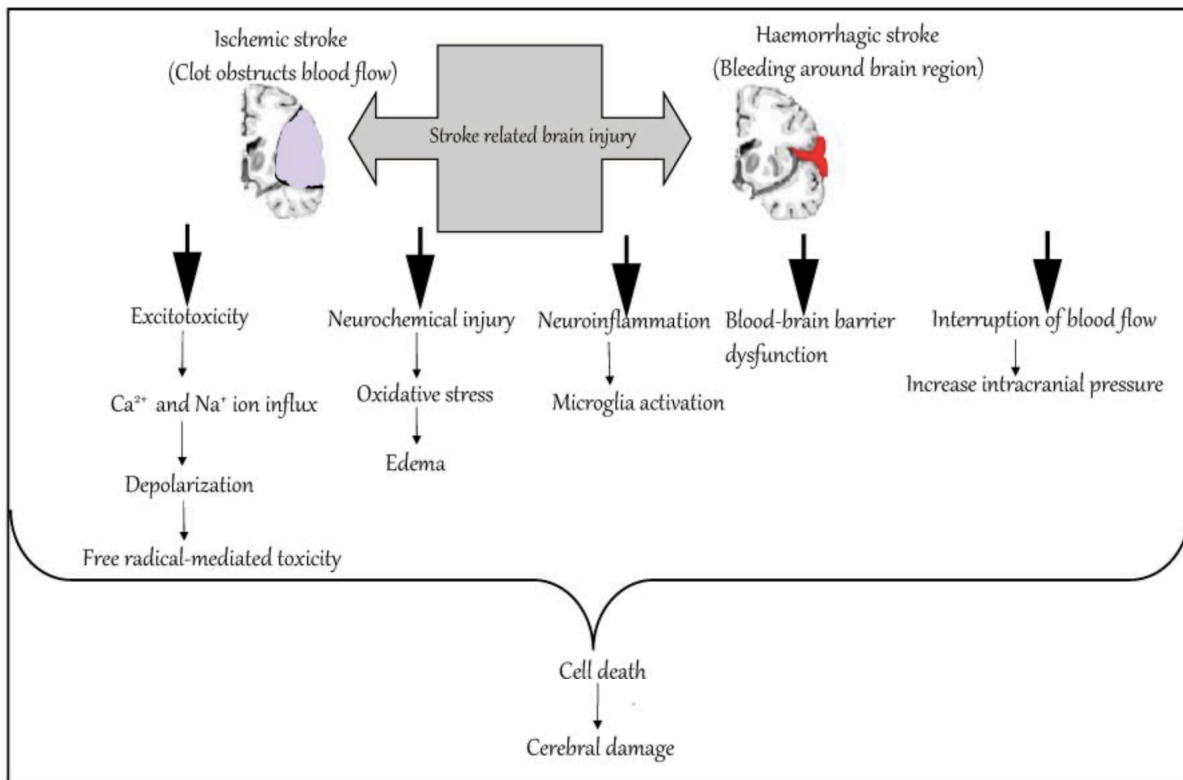


Figure 1. The main mechanisms involved in both ischemic and hemorrhagic stroke-related events. During hemorrhagic stroke, the blood supply to the brain is interrupted resulting in blood-brain-barrier (BBB) dysfunction and increased intracranial pressure. In ischemic stroke, blocked blood flow results in excitotoxicity and ion imbalance which causes depolarisation and excessive ROS release. It also results in neurochemical injury where oxidative stress causes edema. All these events cause neuroinflammation marked by microglia activation which together results in cell death and cerebral damage (taken from Kuriakose & Xiao, 2020).

Excitotoxicity is characterised by an over-depolarisation of N-methyl-D-aspartate receptors (NMDARs) on postsynaptic neurons which contribute to the production of reactive oxygen species (ROS) which damage mitochondrial function and lead to cell death (Feske, 2012). Therefore, during the ischemic stroke, there is an energy disruption as adenosine triphosphate (ATP) production is damaged. As a result, ionic gradients maintained by ion channels across neuronal plasma and organelle membranes become disrupted (Putten et al., 2021) leading to excess influx of Ca^{2+} and Na^{+} ions into neurons. This process activates enzymes promoting the release of glutamate which stimulate NMDARs (Rose et al., 2020) and also increases proteases, lipases, kinases and endonucleases which results in cellular damage and death (Lipton, 1999).

In the event of neurochemical injury, induced by oxidative stress, there is a disruption of oxidant-antioxidant balance, particularly in brain cells rich in polyunsaturated fatty acids. Contributing factors include elevated oxidative metabolism, increased levels of prooxidants such as

iron and reduced antioxidant defenses (Pawluk et al., 2022). The increase of ROS damages cell membranes which in turn damages endothelial cells and BBB walls, hence, allowing extra fluids, plasma proteins and other substances to overflow the brain tissue, resulting in edema (Woodruff et al., 2011).

Neuroinflammation is a key contributor in ischemic stroke involving both innate and adaptive immune responses. Brain injury triggers necrosis and apoptosis which in turn initiate an inflammatory cascade mediated by ROS, chemokines and cytokines. This response engages various immune cells including microglia and lymphocytes leading to neuronal damage and cell death (Shaheryar et al., 2021).

Apoptosis is a form of programmed cell death that plays a significant role in neuronal loss during ischemic stroke. It is triggered by intrinsic or extrinsic pathways. The intrinsic pathway is initiated by oxygen and nutrient deprivation which impairs ATP production leading to ionic imbalances, intracellular Ca^{2+} accumulation and glutamate excitotoxicity. This cascade activates cytotoxic mechanisms including Calpain activator, ROS generation, membrane damage and DNA fragmentation (Tuo et al., 2022). The extrinsic pathway is driven by inflammatory signaling from glial cells in response to cerebrovascular injury in which key mediators are proinflammatory cytokines and receptors which trigger apoptosis (Xu et al., 2017). In addition to apoptosis, other types of stroke-induced cell death are known as ferroptosis, phagoptosis, parthanatos, pyroptosis and necroptosis (Salaudeen et al., 2024).

Lastly, autophagy is a cellular process responsible for degrading and recycling damaged components and it plays a significant role in ischemic stroke (Kaur & Debnath, 2015). Triggered by oxygen and nutrient deprivation, autophagy is regulated by mechanistic target of rapamycin complex 1 (mTORC1) inhibition and AMP-activated protein kinase activation (Hwang et al., 2017) and it can support cell survival by clearing damaged structures or may contribute to neuronal injury and death if its activation is prolonged (Peng et al., 2022).

2.6. Diagnosis and treatment of stroke

A fast diagnosis of stroke is crucial, because for every minute that the brain is starved during stroke episode, 1,9 million neurons are lost (Powers et al., 2018) and fast recognition of stroke significantly reduces stroke severity, leading to better return to baseline neurological function. In fact, the phrase “**time is brain**” highlights the urgency of immediate evaluation and treatment, as nerve tissue rapidly deteriorates as a stroke progresses (Saver, 2006).

The most basic and widely publicly used identification of stroke is called FAST in which the observer has to inspect the patient for facial drooping, arm weakness, speech difficulty and if any of these symptoms appear, to call emergency services (Musuka et al., 2015). There is another widely

used identification of stroke called “suddens” proposed by the National Institute of Neurological Disorders and Stroke (NINDS). The warning signals of “suddens” include: sudden numbness or weakness in face, arm or leg, particularly on one side of the body; sudden confusion or difficulty speaking and understanding speech; sudden vision problems in one or both eyes; sudden difficulty walking, dizziness or loss of balance and coordination; sudden intense headache with no known cause (Soto-Cámara et al., 2020). In the clinical setting, the diagnosis of stroke is made using a combination of the patient's medical history, clinical examination and neuroimaging techniques.

When it comes to the treatment and management of stroke, the main idea is to reduce risk factors and promote brain repair, neuroplasticity and recovery (see figure 2). However, despite extensive research into stroke treatment, it still remains a big challenge (Kuriakose & Xiao, 2020). Only recently there was one Food and Drug Administration (FDA) and EU approved drug to treat acute ischemic stroke called alteplase, but it can only be administered in a very short time window between 3 to 4,5 hours after stroke onset (Hacke et al., 2008). Some other drugs such as tenecteplase were under investigation and in March 2025 it was approved by the U.S. FDA as safe to use (U.S. Food and Drug Administration, 2025).

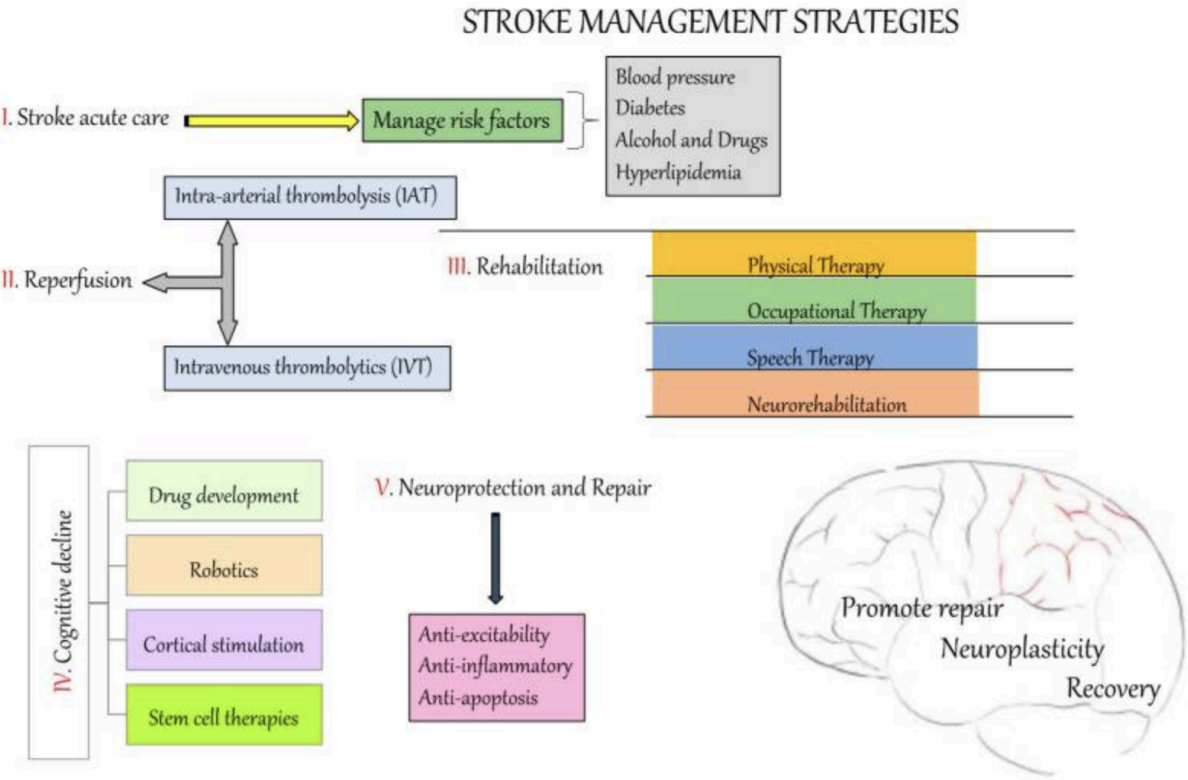


Figure 2. Summary of stroke management strategies, including control of risk factors such as diabetes or high blood pressure, reperfusion therapies including intra-arterial and intravenous thrombolysis and rehabilitation through physical, occupational and speech therapy also including neurorehabilitation. Moreover, cognitive decline can be managed through drug development, robotics, cortical stimulation and stem cell therapies while neuroprotective strategies aim to reduce

excitability, inflammation and cell death. In general, all these strategies aim to support brain repair, neuroplasticity and recovery (taken from Kuriakose & Xiao, 2020).

Recanalisation and reperfusion are the most used treatments when it comes to acute stroke management. Recanalisation can be done with chemical thrombolysis using recombinant tissue plasminogen activator (rtPA) or mechanical embolectomy where the blood clot is removed physically. Reperfusion also plays a vital role, as the penumbra region becomes hypoperfused but not infarcted and it can be saved if blood flow is established by opening occluded arteries. There is evidence that, if administered as promptly as possible after the onset of stroke symptoms, a combination of both intravenous (IV) thrombolysis with rtPA and endovascular thrombectomy can help to improve neurological outcomes (Rabinstein, 2017).

As mentioned above, ischemic stroke activates a cascade of events such as excitotoxic glutamate release, Ca^{2+} overload and neuroinflammation which ultimately lead to cell death via apoptosis and autophagy. With excitotoxicity being a major contributor to neuronal death in stroke, there are specific drugs such as NMDA receptor antagonists that showed neuroprotection in animal models but not in stroke patients due to narrow therapeutic window and side effects (Domercq & Matute, 2019).

Voltage-gated Ca^{2+} channel blockers have demonstrated the ability to reduce ischemic damage in animal models. For the increase of ROS, antioxidants are used in the treatment of acute stroke to reduce or neutralise them, hence, eliminating existing free radicals from the body. Regarding neuroinflammation, anti-inflammatory agents are being used, such as tetracycline derivative minocycline, which crosses BBB and inhibits microglial activation (Hayakawa et al., 2008) as well as oxidative and inflammatory damage (Yong et al., 2001), apoptosis (Power et al., 2003) and excitotoxicity (Tikka & Koistinaho, 2001). Lastly, there are other types of therapies that focus on neuronal repair and regeneration such as stem cell transplantation (Lee et al., 2010), growth factors (Tanake et al., 1995) and rehabilitation.

2.7. Consequences of stroke

While stroke is the leading cause of long-term adult disability and even with improvements in early treatment and rehabilitation, still two-thirds of survivors live with lasting neurological impairments and fewer than 20% return to pre-stroke personal and professional life (Di Carlo, 2009). Motor impairments are the most frequent consequences of stroke, with contralateral limb hemiparesis affecting 80% of survivors and persisting in more than 40% of individuals during the chronic phase (Lee et al., 2015). Upper limb motor dysfunction may present as muscle weakness, altered muscle tone, joint contractures, instability or deficits in motor coordination. These limitations interfere with

everyday activities such as reaching, grasping, holding or using tools (Lang et al., 2013). The recovery of motor function after stroke typically involves a multidisciplinary team that implements a range of evidence-based interventions to support natural functional recovery (Raffin & Hummel, 2018).

Somatosensory impairment is also a common consequence of stroke which occurs in more than half of the cases of ischemic stroke (Kessner et al., 2019) but it can be overlooked as motor symptoms are observed more clearly (Sullivan et al., 2008). Somatosensory deficits, following ischemic stroke, are largely influenced by the specific brain regions affected by the infarct (Meyer et al., 2016). Neuroimaging studies have linked these impairments to lesions located in the thalamus, dorsal internal capsule, corona radiata, pons and various cortical areas (Kim, 1992). Voxel-based lesion-behaviour mapping has revealed that damage to secondary somatosensory and insular cortices is particularly associated with light touch impairments (Preusser et al., 2015). Additionally, a cross-sectional cohort study identified two key brain regions known as the sensory component of the superior thalamic radiation and the secondary somatosensory cortex as central to disturbances in sensory modalities such as light touch, pressure, pinprick pain and proprioception (Meyer et al., 2016).

Moreover, cognitive changes are present in up to 72% of patients in the acute stroke phase, though this rate tends to decrease to approximately 30% within three months of stroke onset (Hurford et al., 2013). Some recovery in cognitive function can occur during the first year, however, many stroke survivors continue to experience cognitive decline, particularly in memory and executive functions (Sachdev et al., 2004). The most commonly impaired cognitive domains following stroke include attention (48,5%), language (27%) including aphasia, short-term memory (24,5%) and executing functioning (18,5%) (Leśniak et al., 2008). Regarding executive functions, planning, initiating tasks, maintaining focus, setting priorities and organising actions toward specific goals may be interfered (Keil & Kaszniak, 2002).

2.8. Animal models of ischemic stroke

Various animal models are being used to study stroke as obtaining human samples with stroke pathophysiology is a challenge due to the unpredictability of stroke onset, delayed arrival at the hospital, ethical limitations as it is not possible to induce stroke, limited access to living brain tissue and variability in patients due to age, genetics, lifestyle and comorbidities. Therefore, animal models allow the stroke to be induced with precise control of the timing and location, access brain tissue for analysis and study stroke mechanisms in real-time, hence enhancing understanding of the pathophysiology of stroke and enabling development of different treatment therapies (Fluri et al., 2015).

Moreover, when working with animals, it is important to follow the **3Rs + reuse** concept which stands for replacement, reduction, refinement and also ethically reuse of animals in research. In 1959 the 3Rs concept was first introduced by Russell and Burch (Russell et al., 1959) after the discussion in 1947 at Universities Federal of Animal Welfare (UFAW) Symposium (Worden, 1947), which is still significant nowadays. It mainly aims to replace animal models with alternative methods. However, when it is not feasible, the smallest number of animals should be used, applying the findings of similar studies. Additionally, all the pain, stress and suffering must be minimised both during experiments and in general animal housing and care.

Most of the experiments are being done with small animals like mice, rats and rabbits while the transient or permanent **middle cerebral artery occlusion (MCAo)** in mice is the most common model used in ischemic stroke research. **Transient (tMCAo)** model involves occlusion of the common carotid artery (CCA), followed by suture insertion into the internal carotid artery (ICA) to block blood flow to MCA (see figure 3) (Merino-Serrais et al., 2023). Common occlusion times are 60, 90 and 120 minutes, or permanent occlusion, with infarcts induced in approximately 88% to 100% of cases (Liu et al., 2009). In mice, infarct volume strongly depends on occlusion duration where extending from 15 to 30 minutes increases infarct size five times (McColl et al., 2004), whereas occlusion below or equal to 10 minutes shows no visible infarction (Fluri et al., 2015). In mice, MCA occlusion results in widespread infarction affecting the cortex, striatum, thalamus, hippocampus and subventricular zone, closely resembling the pattern observed in rat models (Maeda et al., 1999).

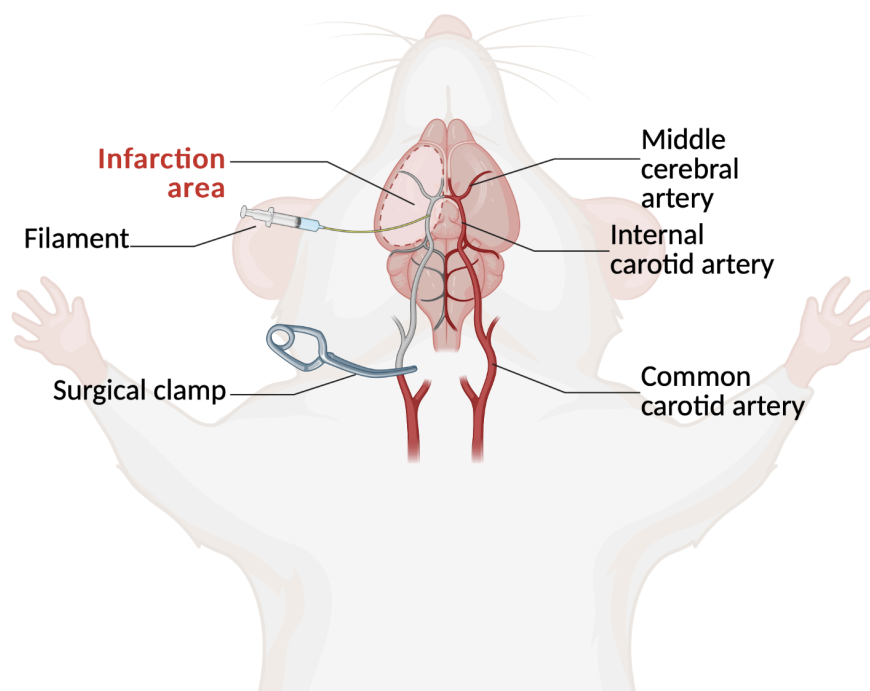


Figure 3. Illustration of a MCAo occlusion procedure in mice (created in <https://BioRender.com>).

Lesion reproducibility is affected by vascular territory, suture diameter (Türeyen et al., 2005), suture length and suture tip (Zarow et al., 1997). Interestingly, stroke size varies by rodent strain (Duverger & MacKenzie, 1998; Cheng et al., 2012) but the size of penumbra appears to stay the same no matter the rodent strain (Reid et al., 2012). This model closely replicates human ischemic stroke and it allows precise control of ischemia duration, is quick and simple to perform and produces consistent infarct volumes. It also models stroke pathophysiology processes such as neuronal death, inflammation and BBB damage (Howells et al., 2010), which is extremely useful in treatment research.

Another used model that also involves the occlusion of MCA is called the **craniectomy model**. The surgical method for MCA occlusion involves a craniectomy and dura opening to access the artery. Here, two main techniques are used. In one, MCA is permanently or temporarily blocked after removing the zygomatic arch and skull over it directly with electrocoagulation (Tamura et al., 1981) or with microaneurysm clips which lift MCA from the brain and hence, disrupt the blood flow (Shigeno et al., 1985). In another, known as the three-vessel occlusion (3VO) model, CCAs are blocked to reduce collateral blood flow and worsen ischemia (McAuley, 1995). However, this model mainly affects the cortex and white matter, but not deeper structures (Buchan et al., 1992). The main advantages of this model include high reproducibility, low mortality and visible confirmation of artery blockage. However, it can damage the brain and blood vessels, alter BBB function and require advanced surgical skills (Fluri et al., 2015).

The **photothrombotic stroke model** is also being used in research of stroke. It is based on light-induced clot formation following the administration of a photoactive dye, such as Rose Bengal or erythrosin B. After injection of these dyes, targeted brain regions are irradiated through the intact skull with light at a specific wavelength. This method generates reactive oxygen species that cause endothelial damage, platelet activation and thrombosis in cortical vessels (Watson et al., 1985) eventually leading to ischemic cell death (Dietrich et al., 1986). Advantages of this model include minimal surgical interventions, high reproducibility and low mortality, yet, due to rapid and irreversible vessel occlusion, this model lacks an ischemic penumbra and collateral reperfusion which makes it different to human stroke pathophysiology (Provenzale et al., 2003).

The last two models used in stroke research are the **Endothelin-1 (ET-1) model** and the **embolic stroke model**. The ET-1 model induces focal ischemia through a strong vasoconstrictive peptide (Yanagisawa et al., 1988). ET-1 can be delivered to exposed MCA (Robinson et al., 1990), injected stereotactically into the brain (Hughes et al., 2003) or applied to the cortical surface (Fuxe et al., 1997) producing lesions similar to permanent MCAo (Sharkey, 1993). This model offers low invasiveness, low mortality and precise targeting but may activate astrocytes and complicate repair

due to ET-1 receptor presence in neurons and glia (Nakagomi et al., 2000; Uesugi et al., 1998; Carmichael, 2005).

Emboic models include microsphere/macrosphere and thromboembolic clot models. Microspheres cause multifocal infarcts (Carmichael, 2005) while macrospheres block MCA without affecting the hypothalamus (Gerriets et al., 2003). Thromboembolic models use autologous clots that better replicate human stroke and enable testing of thrombolytics but infarct size variability and spontaneous reperfusion are challenges (Niessen et al., 2003; Overgaard, 1994; Wang et al., 2001).

Despite promising neuroprotective results in animal models, most therapies have failed in clinical trials, largely due to differences in experimental design, including treatment timing and the use of young, healthy animals unlike typical human stroke patients (Dirnagl & Macleod, 2009). Using models with more clinically relevant features and optimising preclinical study design could improve the translation of stroke treatments to human patients. (Hossmann, 2012).

2.9. Brain anatomy and lateralisation

Cerebral cortex is the largest part of the brain and it plays a main role in the control of higher-order cognitive processes such as perception, language, decision-making and motor planning. Anatomically, it is divided into left and right hemispheres by **longitudinal fissure** and both hemispheres are able to communicate with each other with the help of **corpus callosum** which is located between the hemispheres and anterior commissure. The cerebral cortex is divided into the neocortex, also known as the isocortex and the allocortex. The allocortex includes evolutionarily older regions like the hippocampus and olfactory cortex and occupies a larger cortical area in lower mammals such as rodents. The neocortex dominates the human brain and has a six-layered structure that emerges during development (Cadwell et al., 2019).

Anatomically, cerebral cortex has four lobes: **frontal** which is responsible for executive processes such as attention, planning, sequencing, motor function and action regulation; **temporal** which plays a key role in hearing perception, learning, memory and emotional regulation; **parietal** which processes somatosensory information and **occipital** which handles visual information. In between the temporal and frontal lobe there is an **insular cortex** which is responsible for taste, visceral and vestibular information, equilibrium and autonomic control. Also, deep within the brain there is a **limbic lobe** which involves amygdala, hippocampal formation and hypothalamus, which are all responsible for learning and memory, emotions and smell (Stirling, 2000).

The human brain demonstrates hemispheric specialisation, also known as **brain lateralisation**, where the left and right hemispheres are each adapted to process different types of sensory information, manage distinct motor functions and attend to specific cognitive tasks (Rogers, 2021). For example, the left hemisphere is more involved in language processing, speech, reading and

writing. It also handles logical thinking, whereas the right hemisphere is more involved in spatial abilities, facial recognition, sound perception and emotional processing (Hartwigsen et al., 2021).

2.10. Cortical areas and subcortical structures

The cerebral cortex is functionally divided into specialised cortical areas that process distinct types of information. The **primary motor cortex**, which is primarily located in the precentral gyrus of the frontal lobe, gives rise to the corticospinal tract and is responsible for the execution of voluntary movements. Damage here may result in movement deficits such as weakness or paralysis on the opposite side of the body. The **primary auditory cortex**, located in the superior temporal gyrus of the temporal lobe, receives thalamic input and processes auditory information. Damage in this region on one side of the brain has a small effect on hearing (Vanderah & Gould, 2022). The **primary somatosensory cortex**, which is found in the postcentral gyrus of the parietal lobes, receives inputs from thalamic relay nuclei and processes tactile sensory input from the body, such as touch, pressure and proprioception. Damage in this region may lead to reduced tactile sensitivity (Stirling, 2000). The **primary visual cortex**, situated in the occipital lobe, is the main center for processing visual information. These regions are organised hierarchically, where primary areas handle basic processing. Interestingly, damage to this area may result in almost complete loss of awareness of visual stimuli.

There are also **secondary**, **tertiary** and **associative areas** that receive bilateral input from primary areas, further integrating the data. The secondary and tertiary cortical areas are located adjacent to their respective primary areas and processes superior analysis of received stimulus. The association cortical areas are not connected to a single sensory modality, yet, they integrate information across multiple senses (Vanderah & Gould, 2022).

The cortical structures together with subcortical structures such as corpus callosum, amygdaloid complex, thalamus, hypothalamus, hippocampal formation and dorsal striatum will be analysed in the current work. As mentioned previously, **corpus callosum** is a white-matter structure, located between the two hemispheres, serving as a gateway for interhemispheric communication. The **amygdaloid complex**, which is involved in emotional processing and especially fear response, is located in the medial temporal lobe and is made of around 13 nuclei which all make intra and inter-connections and which can further be subdivided into three main groups: basolateral, cortical and centromedial (Sah et al., 2003). The **thalamus**, located deep within the forebrain, is made up of over 50 nuclei and is a crucial structure for consciousness as it relays sensory signals, regulates arousal from the brainstem and maintains cortical connections (Mashour & Pryor, 2015). The **hypothalamus**, being one of the oldest structures in the brain, is located below thalamus. The main role of it is to maintain basic functions or homeostasis such as thermoregulation, feeding and energy

metabolism and sleep and wakefulness (Saper & Lowell, 2014). The **hippocampal formation** which is located in the medial ventral temporal lobe is made of the hippocampus, dentate gyrus and subiculum. It is essential for memory, especially episodic, short-term, working memory and memory consolidation. It mainly receives input from the entorhinal cortex which receives information from association areas, suggesting that memories are stored in association and primary cortices (Drake et al., 2023). The **dorsal striatum**, which is part of the corpus striatum, is made of caudate nucleus and putamen. It plays a direct role in decision-making when selecting and initiating actions as it integrates sensorimotor, cognitive and emotional information through corticostriatal circuits (Balleine et al., 2007).

Together, these cortical and subcortical regions form a complex network supporting essential sensory, motor, cognitive and emotional functions.

2.11. Cortical layers, white matter and blood supply

The neocortex is arranged into six horizontal layers which differ in their cell types, size of cell bodies, density, distribution of myelinated fibers and connections (see figure 4).

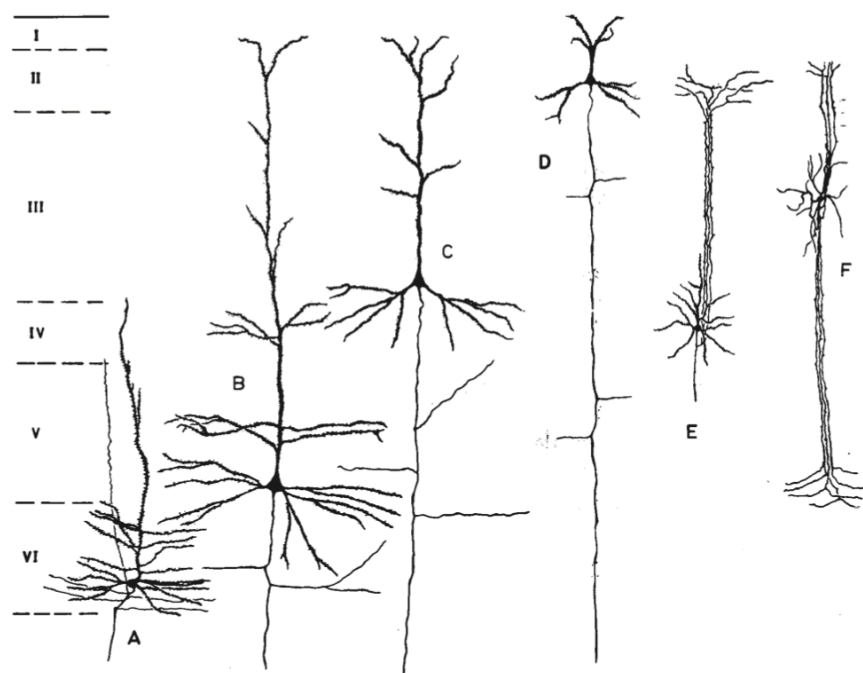


Figure 4. Neuron types across cortical layers I-VI based on classical Golgi staining. **A** shows a small pyramidal neuron from layer VI with apical and basal dendrites. **B**, **C** and **D** are large pyramidal neurons from layers V and IV with long apical dendrites reaching upper layers and basal dendritic arborisation. **E** and **F** represent stellate cells or small interneurons from layers III and IV (taken from Rolls et al., 2016).

Each layer plays a unique role well described by Standring (2021):

- Layer I (molecular layer) is the most superficial cortical layer, characterised by a small cellular density. It is primarily composed of the terminal branches of apical dendrites from deeper pyramidal neurons and horizontally running axons from various origins.
- Layer II (external granular layer) is made of small pyramidal neurons and interneurons. Their apical dendrites extend into layer I, while their axons descend toward deeper layers, especially layer V, forming numerous local connections. It also has thalamo-cortical afferents.
- Layer III (external pyramidal layer) is composed of small to medium size pyramidal neurons. This layer is a principal source of cortico-cortical efferents (from the collateral hemisphere) and thalamo-cortical afferents. Its neurons extend dendrites toward the surface and send axonal branches both within the cortex and to distant cortical areas and subcortical targets like the striatum.
- Layer IV (internal granular layer) contains different types of cells including granular, spiny stellate and pyramidal neurons. This layer is well developed in the primary visual cortex and has thalamo-cortical and intra-hemispheric cortico-cortical projections with the best termination seen in major thalamic input to somatosensory, visual and auditory areas.
- Layer V (internal pyramidal layer) is dominated by large pyramidal cells in which axons from the cortex project to subcortical structures. This layer also has scattered non-pyramidal cells.
- Layer VI (polymorphic or multiform layer) is the deepest cortical layer containing a variety of cells including pyramidal neurons, spiny stellate cells, fusiform cells and inhibitory interneurons. Neurons in this layer primarily project back to the thalamus, forming part of reciprocal cortico-thalamic circuits.

Beneath the cortical layers there is a **white matter** (WH), composed of myelinated axons, connecting different parts of the brain. These fibers can be found in the corpus callosum or anterior commissure, forming a network that enables coordinated processing across distributed cortical areas (Standring, 2021).

Moreover, the cerebral cortex is supported by a highly developed vascular system. The major arteries that branch into smaller arterioles and nourish the cells with oxygen and nutrients are the anterior cerebral artery (ACA), the middle cerebral artery (MCA) and the posterior cerebral artery (PCA). The ACA supplies the medial portions of the frontal and parietal lobes including areas involved in motor and sensory functions of the lower limbs. The MCA, being the largest and most commonly involved in ischemic stroke (Treadwell & Thanvi, 2010), irrigates the lateral aspects of the cerebral hemispheres, involving the primary motor and sensory cortices for the face and upper

limbs as well as language areas in the dominant hemisphere. The PCA supplies occipital lobe and therefore is responsible for visual processing and the inferior temporal lobe. Proper cortical irrigation is essential for maintaining neuronal health and function, therefore, disruption in this system can lead to significant neuronal deficits such as the ones observed in ischemic stroke. Interestingly, these arterial territories are interconnected by a network of collateral vessels such as the circle of Willis, which can provide compensatory flow in case of occlusion (Liebeskind, 2003).

2.12. Types of cortical neurons

The cerebral cortex is mainly composed of two broad types of neurons - **excitatory pyramidal neurons** and **interneurons**, each with unique structural and functional roles. Pyramidal neurons are the principal excitatory cells of the cortex, making up about 70-85% of all cortical neurons (Parnavelas, 2002). They have a triangular cell body, a thick and long apical dendrite that extends towards the cortical surface and several basal dendrites spreading laterally. Their axons project to distant cortical or subcortical regions, forming intra-cortical and cortico-spinal projections (Standring, 2021). Their dendrites, covered with spines, integrate a large number of synaptic inputs and contribute significantly to the complexity of neuronal signaling (Merino-Serrais et al., 2023).

Another second most numerous subtype of excitatory but non-pyramidal neurons are the **spiny stellate cells**. These cells have a star-like dendritic shape, use glutamate as their neurotransmitter and receive thalamo-cortical input, playing a critical role in processing sensory information.

In contrast, **cortical interneurons** are smaller, mostly inhibitory with short axons found throughout all cortical layers. They release Gamma-Aminobutyric Acid (GABA) and regulate the activity of pyramidal neurons by forming local circuits. Together, all these neurons form the foundation of cortical processing, enabling a balance between excitation and inhibition which is essential for normal brain function (Standring, 2021).

2.13. Comparison between human and mouse brain

There are a lot of differences and similarities between the human and mouse brain described in great details by Schröder et al (2020).

The human cerebral cortex has folds and sulci which increases the surface area. In the mouse, the cortex is lissencephalic and has a smooth surface, meaning no gyri or sulci. Moreover, humans have clearly identifiable Brodmann areas where sulci and gyri serve as external landmarks such as precentral gyrus containing the primary motor cortex, while due to a smooth surface mice do not have such clearly identifiable features.

When it comes to cortical areas, in the human motor cortex the cortico-spinal tract arises and it is critical for voluntary movement while in mice it is positioned cranially in the precentral area,

comprising primary (M1) and secondary (M2) motor cortices but it is still essential for movement initiation via the cortico-spinal tract.

The somatosensory cortex in humans is organised somatotopically, like a homunculus, with distinct representation of body parts while in mice it is also somatotopically organised, like “musculus” but with representation of the whisker field, especially in the barrel cortex. Other parts like the forelimb, hindlimb and jaw are also represented forming a mouse equivalent of the human homunculus.

The visual cortex in humans is located in the occipital lobe with clear representation of the visual field whereas in mice it is located dorsal to the temporal area with subdivisions into binocular and monocular areas. As Zhuang et al. (2017) found, the retinotopic map in the mouse extends into the retrosplenial cortex and primary somatosensory cortex, showing a broader and less spatially confined representation than in humans (Zhuang et al., 2017).

There are also differences in the hippocampus, amygdala, corpus callosum and striatum. Human hippocampus is located in the ventral part of the temporal lobe and has a hook-like shape while the mouse hippocampus has a banana-like shape, extending dorsoventrally. The location of amygdala is similar in both humans and mice, however, human amygdala is larger and more easily visualised in imaging and sectioning while mouse amygdala is small and harder to distinguish in basic imaging but it can be seen on vibratome sections. The corpus callosum is present in both but in mice it is thinner and carries fewer fibers. Finally, striatum in humans is divided into a caudate nucleus and putamen by the internal capsule while in mice it is a single, solid structure called caudate putamen, which is not separated by internal capsule. In rodents, experimentally induced strokes are common in the internal capsule, severely damaging major sensory and motor pathways (Schröder et al., 2020).

2.14. Cortical alterations after ischemic stroke and diaschisis

The cortical and functional alterations following ischemic stroke depend on the brain location where the stroke occurred and the time it was happening, as the longer the time of stroke, the more severe damage. For example, if a lesion has occurred on the left side of the hemisphere, near Broca’s region, there may be language disruption (Dronkers et al., 2007). If a lesion has occurred outside the hippocampus, there may be memory disruptions (Lim & Alexander, 2009). If a lesion has occurred outside the frontal cortex, there may be disruptions in social behaviour (Darby et al., 2018).

WM, which has a lower blood supply compared to other brain regions, is also severely affected in case of stroke due to deprivation of oxygen and nutrients (Iadecola et al., 2009). Indeed, 64 % to 86 % of stroke patients experience white matter injury (WMI) (Li et al., 2013). WMI is also related to

the pathophysiology events of stroke such as oxidative stress (Husain & Juurlink, 1995) and excitotoxicity (Domercq et al., 2007).

However, most functional disorders that occur after stroke are a result of damage in multiple brain regions, in a form of a process known as **diaschisis** (Merino-Serrais et al., 2023). In 1914 the first to mention this term was Monakow. He emphasised, that diaschisis has four aspects: 1) the existence of a localised brain lesion, 2) a reduction or temporary suspension of neural activity in distant regions, 3) disruption of the neural pathways linking the lesion site to these remote areas and 4) a clinical progression that is dynamic in nature but tend to diminish over time (von Monakow, 1914). However, the term remained clinically incomplete until the in vivo autoradiography techniques were invented in the late 1970's which would measure glucose metabolism in the brain (Raichle et al., 1975). The measurements would show reduced metabolism in the distant regions to the lesion hence, becoming an operational definition of diaschisis (Baron et al., 1984). It is now known that diaschisis refers to neurophysiological changes in remote regions from the lesion site, caused by the original damage as the entire neuronal circuit in which that area is involved will be compromised but the effect can be both - decreasing or increasing. Moreover, in case of abnormalities caused by diaschisis, their severity depends on the size and severity of stroke and it can also last from three to four weeks after stroke. A recent modeling work done by Butz et al. (2014) also defines the loss of neural input from the lesion site as deafferentation and supports the idea of network-level changes in diaschisis, as the reorganisation beyond the lesion site happens through homeostatic structural plasticity where neurons adjust their synaptic contacts in order to stabilise disrupted activity (Butz et al., 2014).

Corpus callosum tends to gain a lot of attention here as it connects the two hemispheres and this type of diaschisis can also be called **transcallosal diaschisis** (Reggia, 2004). There were some studies investigating the corpus callosum impact on diaschisis. In 1958 an experiment done by Kempinsky showed that after sectioning corpus callosum, the diaschisis effect was significantly reduced (Kempinsky, 1958). However, Reggia's neurocomputational study has shown that when interhemispheric connections were excitatory there was depression in the contralateral hemisphere, whereas when connections were inhibitory, this effect was absent. This finding highlights that excitation between the two hemispheres is critical in order to model diaschisis (Reggia, 2004).

The whole literature seems to lead to an observation that ischemic stroke leads to both local and distant structural brain alterations, affecting interconnected cortical and subcortical structures as a result of degeneration and/or diaschisis and these findings seem to align with the main objectives of this thesis.

3. Materials and methods

3.1. Animals and sample processing

In this master's thesis, the mice and brain sections used were obtained from the 2019-2020 research project “Multi-scale investigation of synaptic dysfunction after stroke (MISST)”. This project was funded by ERA-NET NEURON (PCI2018-092874, <https://www.era-learn.eu>). As a result of the project, the scientific article “Microanatomical study of pyramidal neurons in the contralesional somatosensory cortex after experimental ischemic stroke” (Merino-Serrais et al., 2023) was published in 2022. Due to their high value and potential for use in other related studies, the remaining brain sections were preserved by freezing, following the protocol established by the Laboratory for Clinical and Cognitive Circuits (LCCC). It also complies with European ethical regulations (3R + Reuse).

The experiment was performed on C57BL/6N mice (Charles River Laboratories), 20 weeks old, 20-22 g that were housed in a 12-hour light/dark cycle, with water and food. At week 10, the mice were divided into 2 groups:

- In the tMCAo group, mice underwent operation. During the operation, mice were anesthetised with 4% isoflurane and kept with 1,5%-2% isoflurane for the whole procedure. For 60 minutes, the left middle cerebral artery was occluded with an inserted siliconized nylon microfilament, which resulted in transient cerebral ischemia (tMCAo) (see figure 5), monitored through a laser Doppler probe that was placed superficially over the left parietal lobe, occupying the territory of the middle cerebral artery. The wounds were treated by povidone-iodine, sutures were performed and mice were taken to a recovery incubator kept at 32°C, allowing motor recovery from anesthesia. After the recovery, mice were transferred back to their home cage where they received postoperative care.
- In the SHAM group, which served as control, mice underwent the same procedure without the insertion of microfilament used for occlusion and received the same postoperative care.

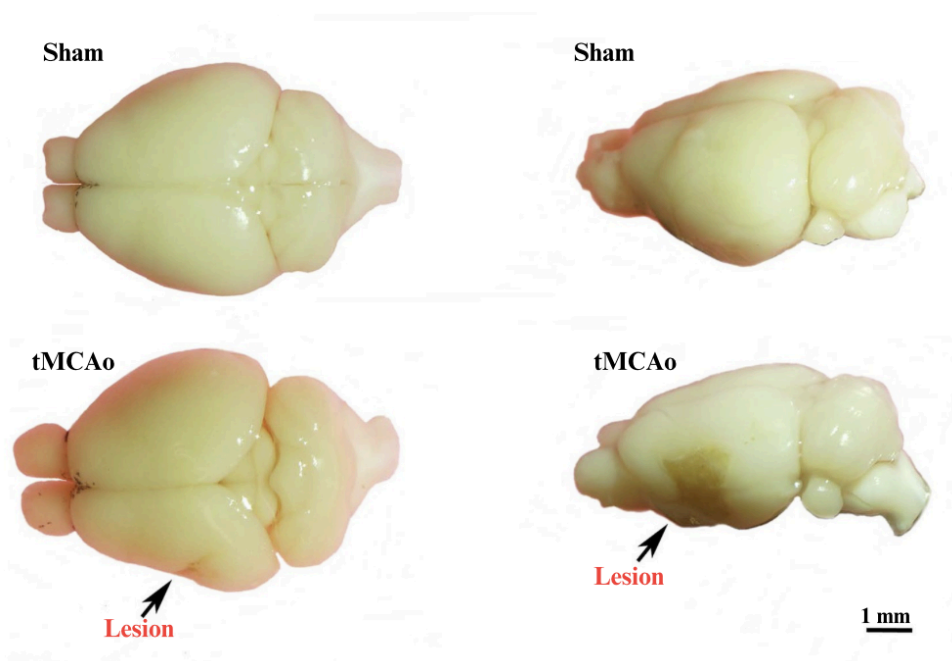


Figure 5. Illustration of a lesion location in tMCAo mice on a left hemisphere, indicated by an arrow (modified from Merino-Serrais et al., 2023).

At 12 weeks after the operation, tMCAo and SHAM mice were sacrificed by perfusion. Mice were anesthetised by intraperitoneal injection with an overdose of sodium pentobarbital and perfused intracardially with phosphate-buffered saline (PBS) for 30-50 ml per animal to remove blood and phosphate buffer pH 7,4 followed by an 80 ml per animal of 4% paraformaldehyde (PFA). The mice's brains were extracted and immersed in PFA for 24 hours. Then, slices of 50 μm and 150 μm thickness were made using a vibratome (LEICA VT1200S) along the anterior-posterior axis of the brain and coronal sections were obtained.

3.2. Sample selection and Nissl staining

In order to observe an ischemic lesion, double Nissl staining was performed on 50 μm thickness brain sections. This method allows the visualisation of neuronal somas by staining cellular elements such as Nissl bodies - clusters of rough endoplasmic reticulum containing a high concentration of ribosomes. For the realization of this Master's thesis, the sections for Nissl staining were selected for both groups: Sham ($n = 9$) and tMCAo ($n = 11$). In order to analyse selected structures, Bregma intervals were selected for simplicity, named L1, L2 and L3, using the stereotaxic mouse brain atlas by Paxinos and Franklin (2001): L1 - from +1.10 to +0.62 mm (see figure 6), L2 - from -0.94 to -1.46 mm (see figure 7), and L3 - from -2.18 to -2.70 mm (see figure 8). The selected sections in some cases were more than one for each animal per interval. These intervals were chosen due to the limited availability of sections, which made it difficult to use the exact same Bregma coordinate for

each of the three representative levels of interest. All layers were further compared with the interactive Allen Institute Brain Atlas (<https://atlas.brain-map.org/>).

Selected sections were washed with PB buffer 0,1M 3 times for 10 mins on a vibrating plate (Heidolph Unimax 1010) and placed in gelatin-coated slides. The sections were then air-dried for 24 hours and dehydrated in 70% ethanol (ETOH) overnight in order to clean the tissue and remove fat. The next day, sections were washed twice in dH₂O (5 min/pass) to rehydrate them and to ensure the removal of ETOH. Then, the sections were stained for 15 minutes in 1% Toluidine blue (pH 4), an acidic dye that marks nucleic acids and then rinsed with dH₂O, following three 5-minute passes. After this, a dehydration process followed using ETOH at a progressive concentration (70%/2 min; 90%/2 min; 99%/2 min). It was then submerged into Xylene for 5 minutes and rehydrated again by ETOH but in decreasing concentrations (99%/2 min; 96%/2 min; 70%/2 min).

The slides were then washed in dH₂O for 1 minute and submerged in Toluidine blue for 15 minutes. After staining, samples were washed with dH₂O, with 3 passes of 5 minutes, with a final dehydration in ETOH (70%/30 sec; 96%/1,5 min; 99%/5 min). Lastly, slides were submerged in Xylene by 2 passes of 7 minutes and the sections were mounted with DePeX and covered with cover glass.

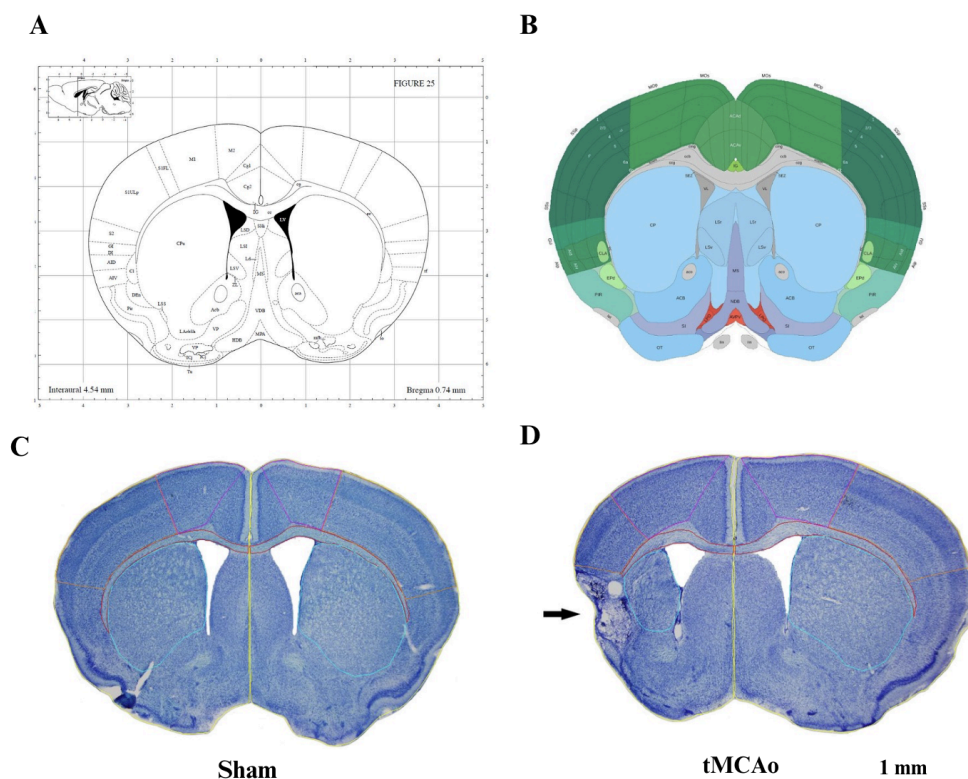


Figure 6. Illustration of an ischemic lesion. (A) An example of Paxinos Brain Atlas figure 25 (Paxinos & Franklin, 2001). (B) An example of Allen Institute (<https://atlas.brain-map.org/>) adult mouse brain atlas figure interval 43-49. (C, D) Nissl stained coronal sections of Sham and tMCAo

brain with measured areas indicated by colours: yellow - hemispheres, red - corpus callosum, purple - motor cortex, orange - somatosensory cortex, blue - striatum.

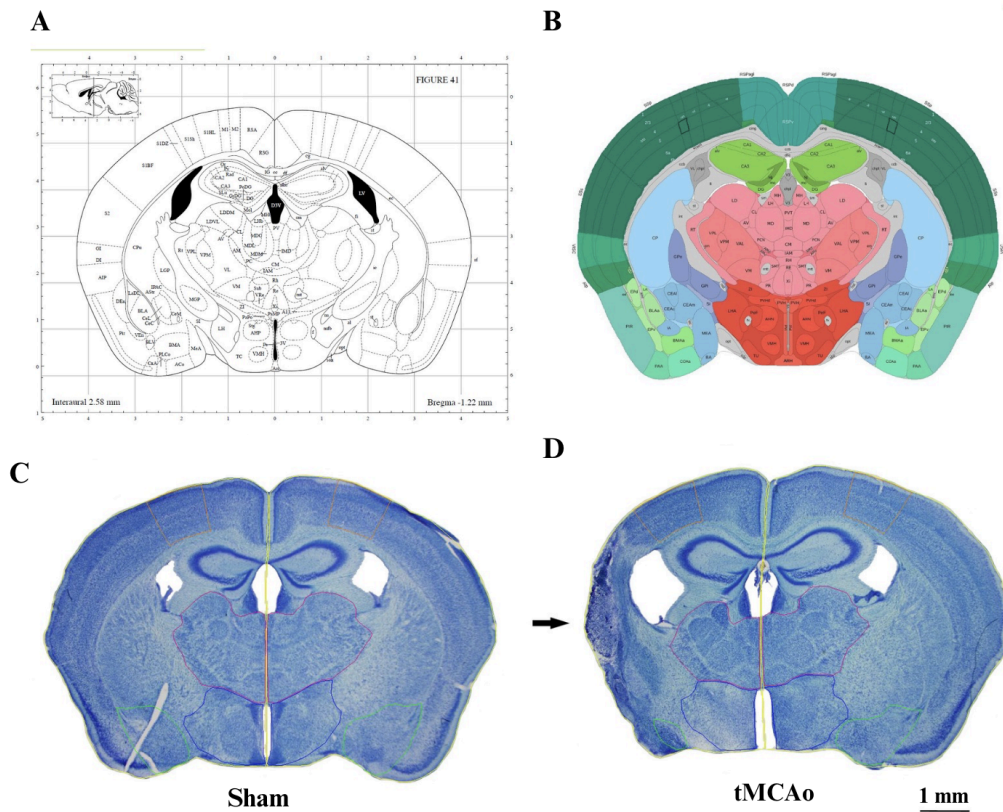


Figure 7. Illustration of an ischemic lesion. (A) An example of Paxinos Brain Atlas figure 41 (Paxinos & Franklin, 2001). (B) An example of Allen Institute (<https://atlas.brain-map.org/>) adult mouse brain atlas figure interval 62-68. (C, D) Nissl stained coronal sections of Sham and tMCAo brain with measured areas indicated by colours: yellow - hemispheres, orange - somatosensory cortex, blue - hypothalamus, green - amygdaloid complex, pink - thalamus.

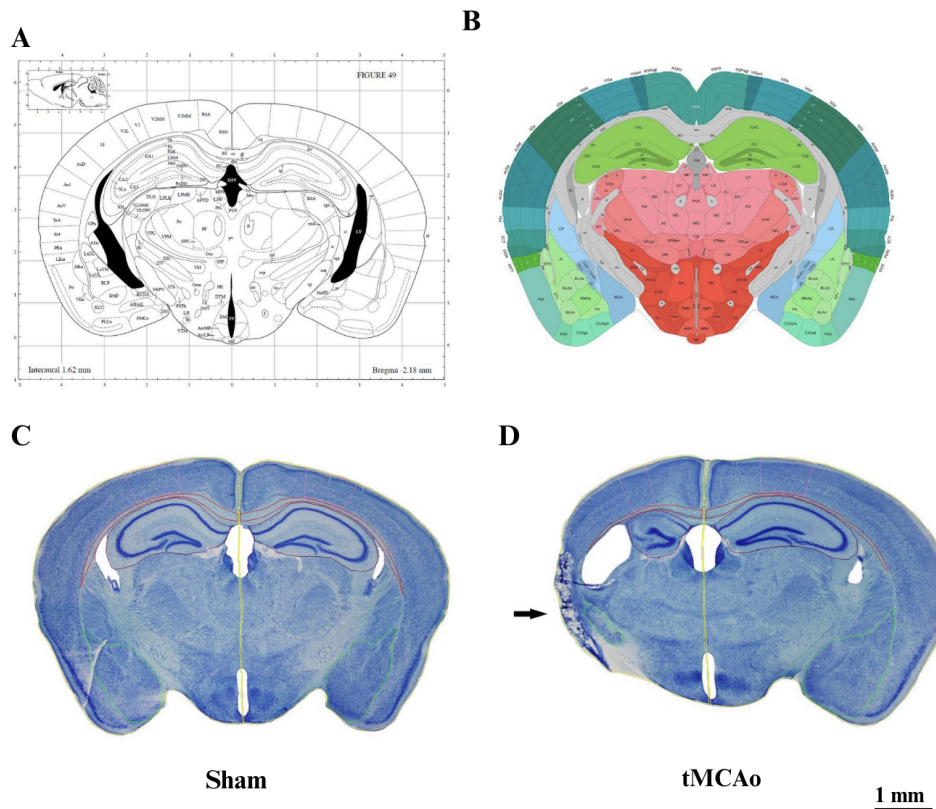


Figure 8. Illustration of an ischemic lesion. (A) An example of Paxinos Brain Atlas figure 49 (Paxinos & Franklin, 2001). (B) An example of Allen Institute (<https://atlas.brain-map.org/>) adult mouse brain atlas figure interval 74-79. (C, D) Nissl stained coronal sections of Sham and tMCAo brain with measured areas indicated by colours: yellow - hemispheres, red - corpus callosum, green - amygdaloid complex, pink - visual cortex, brown - hippocampal formation.

3.3. Estimation of brain areas and thickness

For the analysis of brain structures, the Nissl stained coronal sections were used from both tMCAo and SHAM groups and analysed using images that were taken with an optical microscope (Olympus BX510) with ocular (WH10X/22), lens (PlanApo 1,25x/0,04) and camera (Olympus DP70). Therefore, the images obtained were 12,5 times larger than the tissue sample and had a scale factor of 3,397 ($\mu\text{m}/\text{pixel}$) and image dimension of 4080 x 3072. All image files used were encoded. The areas of interest in the left and right sides - hemispheres, corpus callosum, somatosensory cortex, motor cortex, visual cortex, dorsal striatum, thalamus, hypothalamus, amygdaloid complex and hippocampal formation were being visualised and analysed through NeuroLucida 360 (version 2024.2.2, MBF Bioscience, MicroBrightField, LLC) with functions “contour tracing” and “measure line”. Thickness was measured only for cortical structures and hippocampal formation. Data from the tracings were extracted using NeuroLucida NeuroExplorer. The calculated data were obtained as the total area (mm^2) and thickness (mm) mean.

3.4. Statistical Analysis

NeuroLucida NeuroExplorer software was used to extract the data from NeuroLucida tracings. All statistical calculations were performed using GraphPad Prism 5 (GraphPad Software, San Diego, CA, USA). When groups were compared, pairwise analysis was used, using the non-parametric Mann-Whitney test as it is the most restrictive test. All data were presented as mean \pm SEM. Sample selection by Bregma intervals (L1 - from +1.10 to +0.62 mm, L2 - from -0.94 to -1.46 mm, and L3 - from -2.18 to -2.70 mm) may have increased variability in the results and potentially weakened the statistical correlations.

In the future, ultrastructural analysis of these tissues using electron microscopy is planned. Therefore, the results obtained in this thesis will be valuable in guiding the selection of brain regions for further investigation, as they help identify areas where post-stroke changes are most prominent.

4. Results

4.1. Alterations in total area of both hemispheres and corpus callosum

A non-parametric Mann-Whitney test was used to look for significant differences in the total area in ipsilateral Sham (left) and contralateral tMCAo (right) hemispheres as well as corpus callosum (see table 1 and figure 9).

For hemispheres, the total area was measured for all Bregma intervals L1, L2 and L3.

For the **right hemisphere** at L1, a significant increase in total area was seen in tMCAo group (Sham $17,736 \pm 0,659 \text{ mm}^2$, tMCAo $19,953 \pm 0,749 \text{ mm}^2$, $p = 0,0355$) representing a 12,5% increase compared to Sham group.

Similarly, for L2 and L3 significant increases in total area were also seen. For example, at L2 the tMCAo group showed a significant difference from Sham (Sham $22,682 \pm 0,509 \text{ mm}^2$, tMCAo $24,903 \pm 0,618 \text{ mm}^2$, $p = 0,0274$), showing a 9,79% increase from Sham. At L3 significant increase was seen in tMCAo group (Sham $23,894 \pm 0,283 \text{ mm}^2$, tMCAo $25,894 \pm 0,749 \text{ mm}^2$, $p = 0,0409$) with a 17,41% increase compared to Sham group (see table 1 and figure 9 (A)).

For the **left hemisphere**, a significant reduction in total area was seen across all Bregma intervals in the tMCAo group. At L1 there was a significant decrease in total area in tMCAo (Sham $17,075 \pm 0,638 \text{ mm}^2$, tMCAo $12,871 \pm 0,472 \text{ mm}^2$, $p < 0,0001$) showing a decrease of 24,62% from Sham. At L2 the tMCAo group showed a significant reduction of 21,48% in total area compared to Sham (Sham $23,052 \pm 0,304 \text{ mm}^2$, tMCAo $18,101 \pm 0,584 \text{ mm}^2$, $p < 0,0001$). Moreover, at L3 a 15,39% decrease in total area was seen in tMCAo group compared to Sham group (Sham $23,784 \pm 0,362 \text{ mm}^2$, tMCAo $20,009 \pm 0,718 \text{ mm}^2$, $p = 0,0006$) (see table 1 and figure 9 (A)).

In **corpus callosum** which was measured at Bregma intervals L1 and L3 the only significant reduction was seen in the left hemisphere at L3 in tMCAo group compared to Sham with a 0,94% decrease (Sham $1,487 \pm 0,078 \text{ mm}^2$, tMCAo $1,473 \pm 0,1 \text{ mm}^2$, $p = 0,0023$) while in L1 there was no statistical difference (see table 1 and figure 9 (B)).

Table 1. Comparison of mean total area measurements for right and left hemispheres, posterior and anterior corpus callosum across different Bregma intervals between Sham and tMCAo groups. The table includes the number of samples (n) for each group as well as p-values obtained from the non-parametric Mann-Whitney test. Statistically significant differences ($p < 0,05$) are highlighted in red. The table also includes SEM values and % difference from the Sham group for each structure.

Right side structures	Bregma interval	Group	n =	Total area (mean, mm ²)	SEM	p value	% difference from Sham
Right hemisphere	L1	Sham	10	17.736	0.659	0.0355	
Right hemisphere		tMCAo	10	19.953	0.749	0.0355	12.50
Right hemisphere	L2	Sham	8	22.682	0.509	0.0274	
Right hemisphere		tMCAo	9	24.903	0.618	0.0274	9.79
Right hemisphere	L3	Sham	12	23.894	0.283	0.0409	
Right hemisphere		tMCAo	9	25.968	0.749	0.0409	8.68
Anterior Corpus Callosum	L1	Sham	10	0.850	0.046	0.6047	
Anterior Corpus Callosum		tMCAo	11	0.855	0.050	0.6047	0.65
Posterior Corpus Callosum	L3	Sham	8	1.510	0.070	0.4119	
Posterior Corpus Callosum		tMCAo	9	1.773	0.100	0.4119	17.41
Left side structures	Bregma interval	Group	n =	Total area (mean, mm ²)	SEM	p value	% difference from Sham
Left hemisphere	L1	Sham	10	17.075	0.638	<0.0001	
Left hemisphere		tMCAo	11	12.871	0.472	<0.0001	-24.62
Left hemisphere	L2	Sham	8	23.052	0.304	<0.0001	
Left hemisphere		tMCAo	9	18.101	0.584	<0.0002	-21.48
Left hemisphere	L3	Sham	9	23.784	0.362	0.0006	
Left hemisphere		tMCAo	10	20.009	0.718	0.0006	-15.39
Anterior Corpus Callosum	L1	Sham	10	0.793	0.040	0.1321	
Anterior Corpus Callosum		tMCAo	11	0.673	0.059	0.1321	-15.14
Posterior Corpus Callosum	L3	Sham	8	1.487	0.078	0.0023	
Posterior Corpus Callosum		tMCAo	9	1.473	0.100	0.0023	-0.94

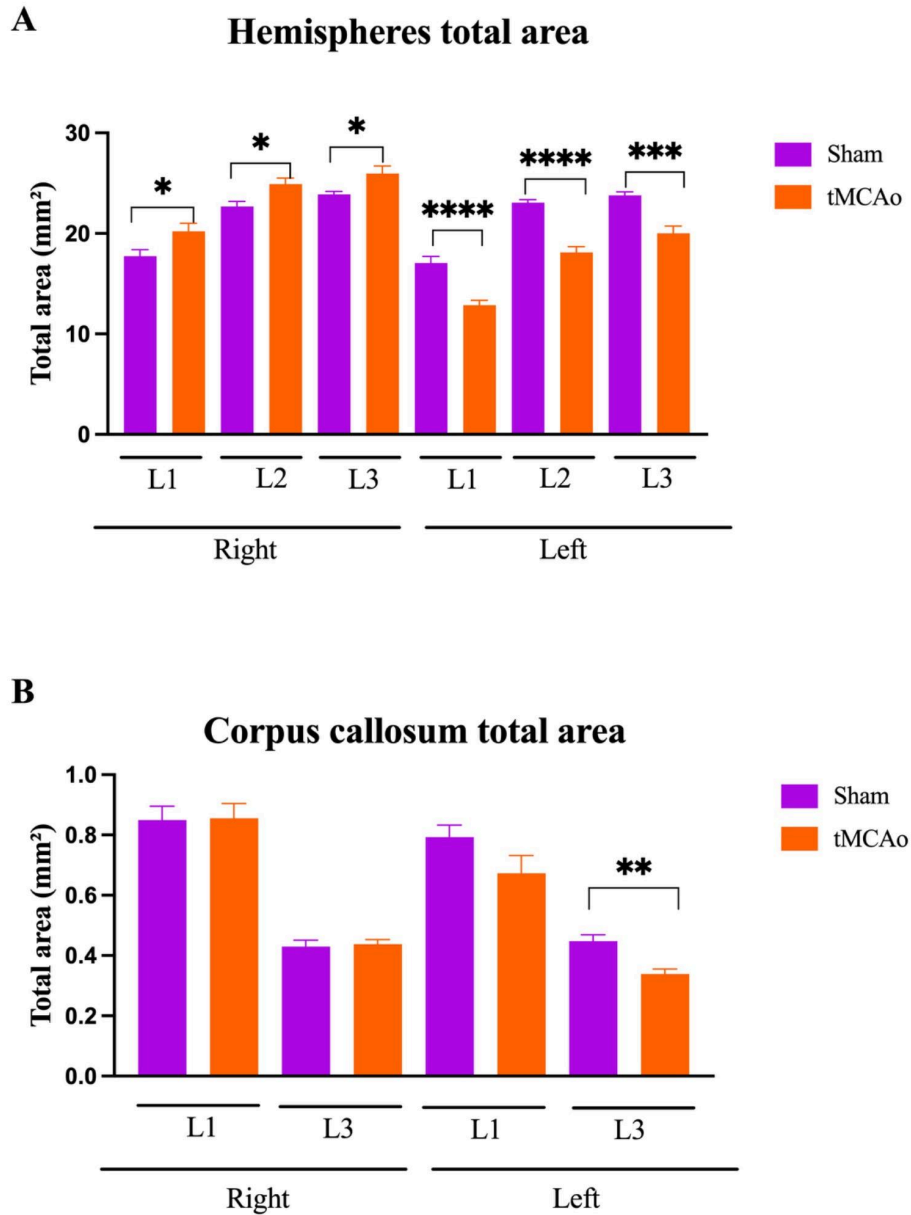


Figure 9. Comparison of total area measurements for both hemispheres and left and corpus callosum at left and right side between Sham and tMCAo groups. **(A)** Total area measurement for right and left hemispheres at L1, L2, L3. **(B)** Total area measurement for right and left corpus callosum at L1, L3. Figures are presented as mean \pm SEM. Statistically significant difference is indicated by asterisk (* $p < 0,05$; ** $p < 0,01$; *** $p < 0,001$; **** $p < 0,0001$) determined by non-parametric Mann-Whitney test.

4.2. Alterations in total area of cortical areas

A non-parametric Mann-Whitney test indicated a significant difference in the total area of all cortical areas between Sham and tMCAo groups (see table 2 and figure 10).

Somatosensory cortex was measured in all Bregma intervals - L1, L2 and L2 and the only significant difference in total area was seen in left hemisphere at L1 between Sham and tMCAo groups indicating a 50,65% decrease from Sham (Sham $2,714 \pm 0,111 \text{ mm}^2$, tMCAo $1,339 \pm 0,122 \text{ mm}^2$, $p < 0,0001$). No statistically significant differences were seen in the left side L2 ($p = 0,2224$) and right side L1 ($p = 0,1517$) and L2 ($p = 0,1135$) (see table 2 and figure 10 (A)).

When it comes to a comparison of the **motor cortex** which was measured in the L1, significant differences were seen in both hemispheres. In the right hemisphere there was a significantly larger total area in the tMCAo group compared to Sham indicating a 84,04 increase from Sham (Sham $1,809 \pm 0,07 \text{ mm}^2$, tMCAo $3,329 \pm 0,187 \text{ mm}^2$, $p < 0,0001$). In the left hemisphere L1, the tMCAo group showed a significantly smaller total area compared to Sham indicating a 32,78% reduction from Sham (Sham $1,993 \pm 0,149 \text{ mm}^2$, tMCAo $1,339 \pm 0,122 \text{ mm}^2$, $p = 0,0028$) (see table 2 and figure 10 (B)).

In the **visual cortex**, only measured at L3, a significant reduction in total area was seen on the ipsilateral side indicating a 8,97% decrease from Sham (Sham $2,324 \pm 0,123 \text{ mm}^2$, tMCAo $2,12 \pm 0,215 \text{ mm}^2$, $p = 0,0041$). On the contralateral side at L3 no significant difference was detected ($p = 0,1333$) (see table 2 and figure 10 (C)).

Table 2. Comparison of mean total area measurements of left and right side cortical areas - somatosensory, motor and visual cortices across different Bregma intervals between Sham and tMCAo groups. The table includes the number of samples (n) for each group as well as p-values obtained from the non-parametric Mann-Whitney test. Statistically significant differences ($p < 0,05$) are highlighted in red. The table also includes SEM values and % difference from the Sham group for each structure.

Right side structures	Bregma interval	Group	n =	Total area (mean, mm ²)	SEM	p value	% difference from Sham
Somatosensory Cortex	L1	Sham	10	3.015	0.132	0.1517	
Somatosensory Cortex		tMCAo	11	3.329	0.187	0.1517	10.43
Somatosensory Cortex	L2	Sham	9	1.007	0.039	0.1135	
Somatosensory Cortex		tMCAo	9	1.100	0.047	0.1135	9.25
Motor Cortex	L1	Sham	10	1.809	0.070	<0.0001	
Motor Cortex		tMCAo	11	3.329	0.187	<0.0001	84.04
Anterior Visual Cortex	L3	Sham	10	2.259	0.111	0.1333	
Anterior Visual Cortex		tMCAo	11	2.415	0.204	0.2333	6.87
Left side structures	Bregma interval	Group	n =	Total area (mean, mm ²)	SEM	p value	% difference from Sham
Somatosensory Cortex	L1	Sham	10	2.714	0.111	<0.0001	
Somatosensory Cortex		tMCAo	11	1.339	0.122	<0.0001	-50.65
Somatosensory Cortex	L2	Sham	9	1.005	0.049	0.2224	
Somatosensory Cortex		tMCAo	9	0.861	0.059	0.2224	-14.38
Motor Cortex	L1	Sham	10	1.993	0.149	0.0028	
Motor Cortex		tMCAo	11	1.339	0.122	0.0028	-32.78
Anterior Visual Cortex	L3	Sham	10	2.324	0.123	0.0041	
Anterior Visual Cortex		tMCAo	11	2.120	0.215	0.0041	-8.79

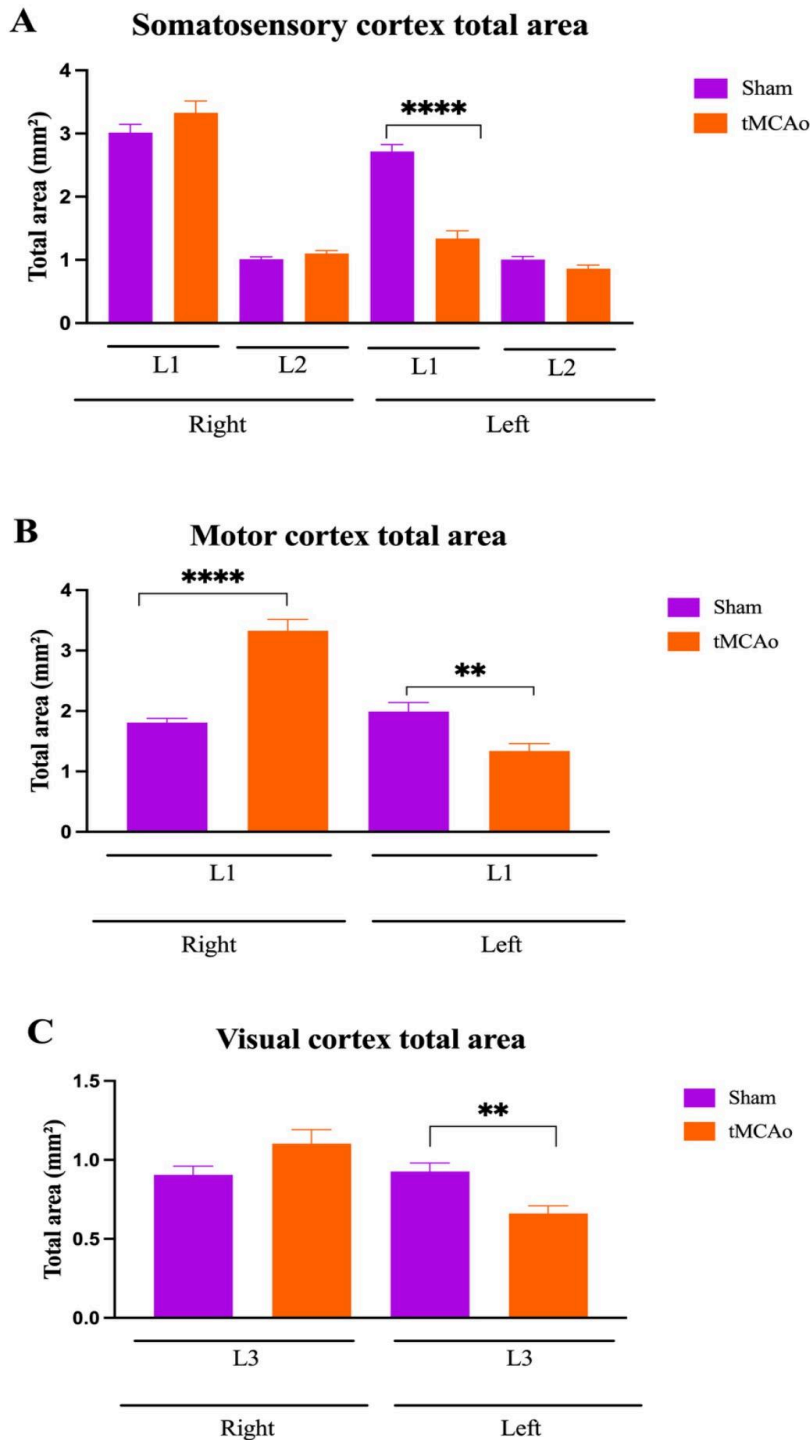


Figure 10. Comparison of total area measurements for cortical structures across different Bregma intervals between Sham and tMCAo groups across left and right hemispheres. **(A)** Total area measurement for somatosensory cortex at L1, L2. **(B)** Total area measurement for motor cortex at L1. **(C)** Total area measurement for visual cortex at L3. Figures are presented as mean \pm SEM. Statistically significant difference is indicated by asterisk (* $p < 0,05$; ** $p < 0,01$; *** $p < 0,001$; **** $p < 0,0001$) determined by non-parametric Mann-Whitney test.

4.3. Alterations in total area of subcortical areas

A non-parametric Mann-Whitney test was used to analyse the differences in total area for all subcortical structures between Sham and MCAp groups and not all structures had statistical differences (see table 1 and figure 11).

The total area of the **amygdaloid complex** was measured in two Bregma intervals - L2 and L3. A statistically significant reduction in total area was found in tMCAo ipsilateral hemisphere on L2 when compared to Sham, representing a 34,56% decrease from Sham (Sham $1,757 \pm 0,17 \text{ mm}^2$, tMCAo $1,15 \pm 0,221 \text{ mm}^2$, $p = 0,0464$). In the same ipsilateral side on L3 a reduction in total area was even more significant in tMCAo group compared to Sham reflecting an 8,97% decrease (Sham $1,72 \pm 0,104 \text{ mm}^2$, tMCAo $1,251 \pm 0,097 \text{ mm}^2$, $p = 0,0005$). On the contralateral side in both L2 and L3 no statistically significant differences were found ($p = 0,1672$ and $p = 0,7103$ respectively) (see table 1 and figure 11 (A)).

Thalamus was measured at Bregma interval L2 and no significant differences in total area were found in both right and left sides of L2 ($p = 0,1139$ and $p = 0,4234$ respectively) (see table 1 and figure 11 (B)).

Similarly, there was no statistically significant difference in the total area of **hypothalamus**, measured at Bregma interval L2, on both sides of hemispheres ($p = 0,1672$ right and $p = 0,3213$ left respectively) (see table 1 and figure 11 (C)).

On top of that, the total area of the **hippocampal formation**, measured at Bregma interval L3, was not significantly different between Sham and tMCAo group in either hemisphere ($p = 0,1564$ right and $p = 0,7802$ left respectively) (see table 1 and figure 11 (D)).

However, a significant reduction in total area of **dorsal striatum**, measured at Bregma interval L1, was seen in the left hemisphere in tMCAo group compared to Sham reflecting a 52,99% decrease (Sham $3,084 \pm 0,286 \text{ mm}^2$, tMCAo $1,45 \pm 0,164 \text{ mm}^2$, $p = 0,0002$). No significant difference was seen in the right hemisphere ($p = 0,2816$) (see table 1 and figure 11 (E)).

Table 3. Comparison of mean total area measurements of left and right side subcortical areas - amygdaloid complex, thalamus, hypothalamus, hippocampal formation and dorsal striatum across different Bregma intervals between Sham and tMCAo groups. The table includes the number of samples (n) for each group as well as p-values obtained from the non-parametric Mann-Whitney test. Statistically significant differences ($p < 0,05$) are highlighted in red. The table also includes SEM values and % difference from the Sham group for each structure.

Right side structures	Bregma interval	⊖ Group	n =	Total area (mean, mm ²)	SEM	p value	% difference from Sham
Amygdaloid Complex	L2	Sham	8	1.564	0.127	0.1672	
Amygdaloid Complex		tMCAo	9	1.760	0.091	0.1672	12.54
Amygdaloid Complex	L3	Sham	9	1.640	0.101	0.7103	
Amygdaloid Complex		tMCAo	9	1.818	0.111	0.7103	10.81
Thalamus	L2	Sham	8	3.289	0.145	0.1139	
Thalamus		tMCAo	9	3.606	0.121	0.1139	9.66
Hypothalamus	L2	Sham	8	1.738	0.084	0.1672	
Hypothalamus		tMCAo	9	1.892	0.067	0.1672	8.81
Hippocampal Formation	L3	Sham	9	3.226	0.238	0.1564	
Hippocampal Formation		tMCAo	9	3.268	0.189	0.1564	1.28
Dorsal Striatum	L1	Sham	10	3.411	0.281	0.2816	
Dorsal Striatum		tMCAo	11	3.871	0.261	0.2816	13.49
Left side structures	Bregma interval	⊖ Group	n =	Total area (mean, mm ²)	SEM	p value	% difference from Sham
Amygdaloid Complex	L2	Sham	8	1.757	0.170	0.0464	
Amygdaloid Complex		tMCAo	9	1.150	0.221	0.0464	-34.56
Amygdaloid Complex	L3	Sham	9	1.720	0.104	0.0005	
Amygdaloid Complex		tMCAo	9	1.251	0.097	0.0005	-27.24
Thalamus	L2	Sham	8	3.234	0.127	0.4234	
Thalamus		tMCAo	9	3.032	0.153	0.4234	-6.26
Hypothalamus	L2	Sham	8	1.808	0.076	0.3213	
Hypothalamus		tMCAo	9	1.672	0.068	0.3213	-7.51
Hippocampal Formation	L3	Sham	9	3.131	0.240	0.7802	
Hippocampal Formation		tMCAo	9	2.831	0.230	0.7802	-9.60
Dorsal Striatum	L1	Sham	10	3.084	0.286	0.0002	
Dorsal Striatum		tMCAo	11	1.450	0.164	0.0002	-52.99

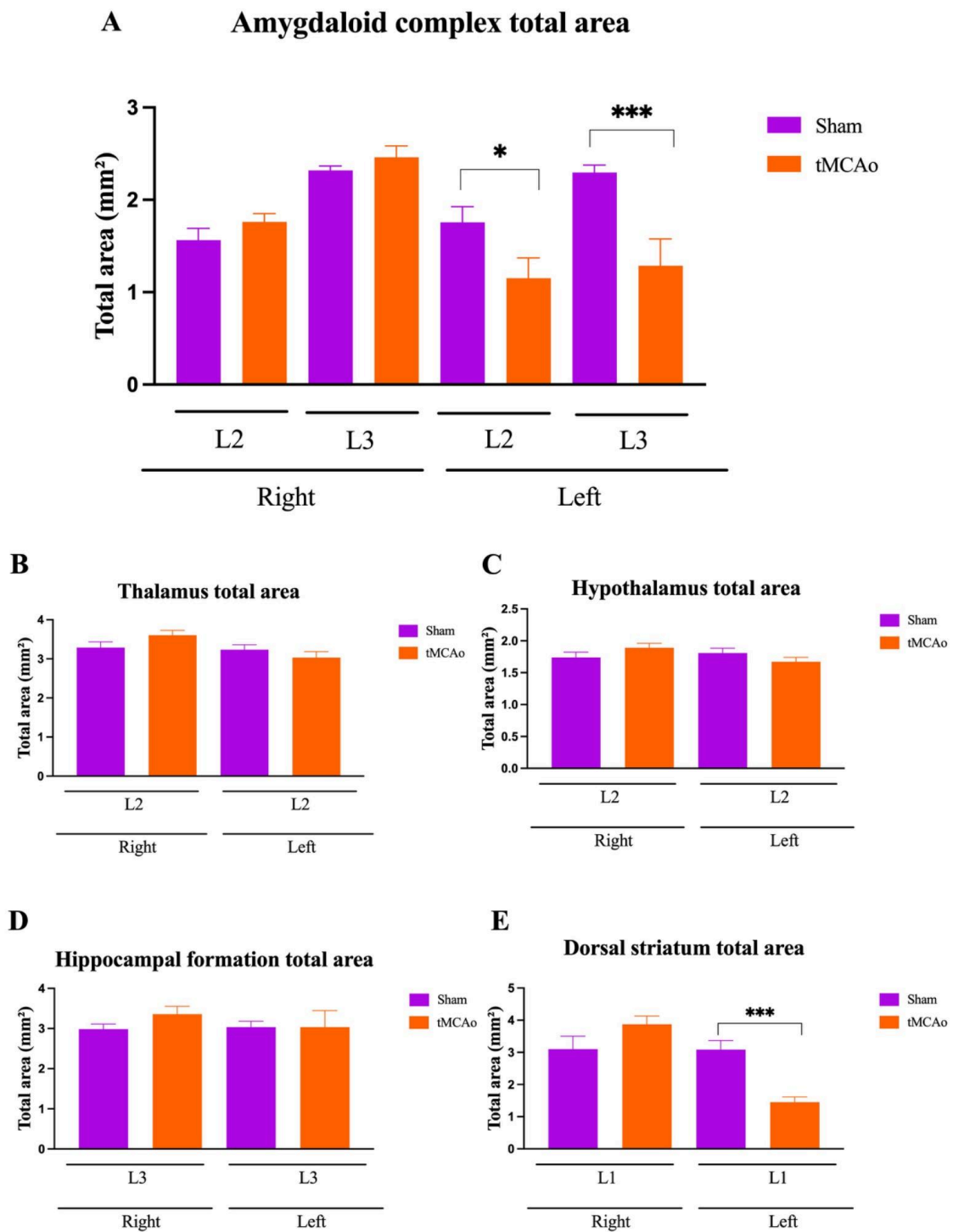


Figure 11. Comparison of total area measurements for subcortical structures across different Bregma intervals between Sham and tMCAo groups across left and right hemispheres. (A) Total area measurement for amygdaloid complex at L2, L3. (B) Total area measurement for thalamus at L2. (C) Total area measurement for hypothalamus at L2. (D) Total area measurement for hippocampal formation at L3. (E) Total area measurement for dorsal striatum at L1. Figures are presented as mean \pm SEM. Statistically significant difference is indicated by asterisk (* $p < 0,05$; ** $p < 0,01$; *** $p < 0,001$; **** $p < 0,0001$) determined by non-parametric Mann-Whitney test.

4.4. Alterations in the thickness of cortical areas and hippocampal formation

A non-parametric Mann-Whitney test was used to look for significant differences in the thickness of cortical areas and the hippocampal formation between Sham and tMCAo groups. Not all structures had significant differences (see table 4 and figure 12).

In **somatosensory cortex**, a significant reduction in thickness was seen in the left hemisphere of L1 in tMCAo group (Sham $1,306 \pm 0,022$ mm, tMCAo $1,122 \pm 0,026$ mm, $p < 0,0001$) representing a 14,09% decrease from Sham. Yet, no significant differences were detected in the right hemisphere at both L1 and L2 ($p = 0,4262$ and $p = 0,4894$ respectively) and also there was no statistical difference in the left hemisphere between Sham and tMCAo groups at L2 ($p = 0,1135$) (see table 4 and figure 12 (A)).

In the **motor cortex**, a significant reduction in thickness was seen in left hemisphere at L1 in tMCAo group when compared to Sham indicating a 16,46% decrease from Sham (Sham $1,343 \pm 0,023$ mm, tMCAo $1,122 \pm 0,026$ mm, $p < 0,0001$). However, on the contralateral side of L1 there were no statistically significant differences in the thickness of a structure ($p = 0,3867$) (see table 4 and figure 12 (B)).

Regarding the **visual cortex**, no significant differences were seen in both Sham and tMCAo groups in either ipsilateral or contralateral side at L3 ($p = 0,0947$ and $p = 0,7197$ respectively) (see table 4 and figure 12 (C)).

Similarly, no significant difference was observed in the thickness of **hippocampal formation** at L3 between Sham and tMCAo groups in either hemisphere ($p = 0,3154$ right and $p = 0,7197$ left) (see table 4 and figure 12 (D)).

Table 4. Comparison of mean thickness measurements for right and left side structures including cortical structures - motor, somatosensory and anterior visual cortex and hippocampal formation across different Bregma intervals between Sham and tMCAo groups. The table includes the number of samples (n) for each group as well as p-values obtained from the non-parametric Mann-Whitney test. Statistically significant differences ($p < 0,05$) are highlighted in red. The table also includes SEM values and % difference from the Sham group for each structure.

Right side structures	Bregma interval	⊖ Group	n =	Thickness (mean, mm)	SEM	p value	% difference from Sham
Motor Cortex	L1	Sham	10	1.305	0.017	0.3867	
Motor Cortex		tMCAo	11	1.31	0.035	0.3867	0.38
Somatosensory Cortex	L1	Sham	10	1.282	0.026	0.4262	
Somatosensory Cortex		tMCAo	11	1.31	0.035	0.4262	2.18
Somatosensory Cortex	L2	Sham	10	1.282	0.026	0.4894	
Somatosensory Cortex		tMCAo	11	1.31	0.035	0.4894	2.18
Hippocampal Formation	L3	Sham	10	1.218	0.023	0.3154	
Hippocampal Formation		tMCAo	11	1.22	0.027	0.3154	0.16
Anterior Visual Cortex	L3	Sham	10	1.187	0.023	0.7197	
Anterior Visual Cortex		tMCAo	11	1.226	0.025	0.7197	3.29
Left side structures	Bregma interval	⊖ Group	n =	Thickness (mean, mm)	SEM	p value	% difference from Sham
Motor Cortex Thickness	L1	Sham	9	1.343	0.023	<0.0001	
Motor Cortex Thickness		tMCAo	11	1.122	0.026	<0.0001	-16.46
Somatosensory Cortex	L1	Sham	10	1.306	0.022	<0.0001	
Somatosensory Cortex		tMCAo	11	1.122	0.026	<0.0001	-14.09
Somatosensory Cortex	L2	Sham	10	1.306	0.022	0.1135	
Somatosensory Cortex		tMCAo	11	1.122	0.026	0.1135	-14.09
Hippocampal Formation	L3	Sham	10	1.246	0.024	0.7197	
Hippocampal Formation		tMCAo	11	1.141	0.026	0.7197	-8.43
Anterior Visual Cortex	L3	Sham	10	1.272	0.029	0.0947	
Anterior Visual Cortex		tMCAo	11	1.181	0.024	0.0947	-7.15

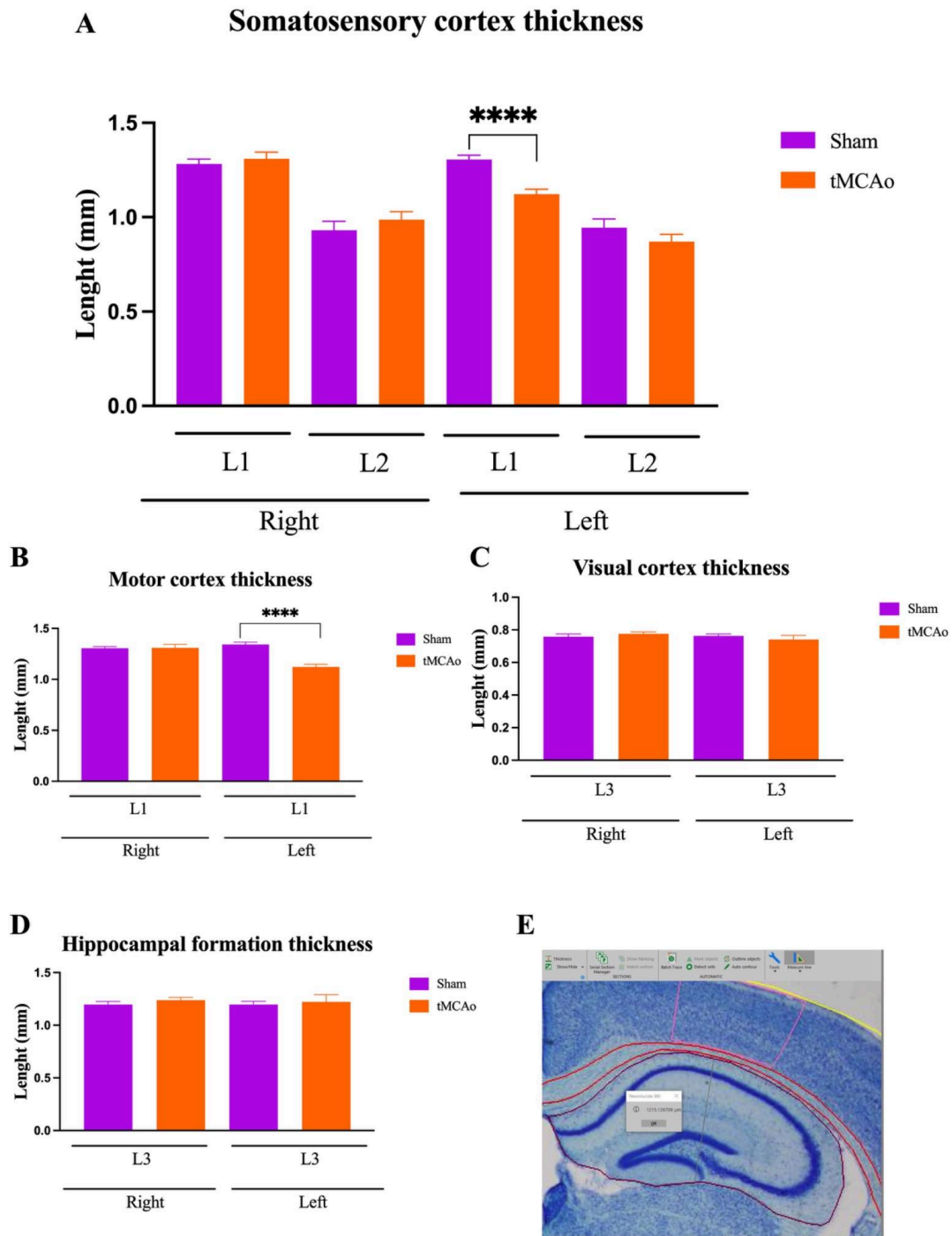


Figure 12. Comparison of thickness (length) measurements for cortical structures and hippocampal formation across different Bregma intervals between Sham and tMCAo groups across left and right hemispheres. (A) Thickness measurement for somatosensory cortex at L1, L2. (B) Thickness measurement for motor cortex at L1. (C) Thickness measurement for visual cortex at L3. (D) Thickness measurement for hippocampal formation at L3. (E) Example of how thickness was measured in NeuroLucida software with function “measure line”. Figures are presented as mean \pm SEM. Statistically significant difference is indicated by asterisk (* $p < 0,05$; ** $p < 0,01$; *** $p < 0,001$; **** $p < 0,0001$) determined by non-parametric Mann-Whitney test.

Discussion

This study investigated anatomical alterations in cortical and subcortical structures using the tMCAo model in mice. The results have shown significant reductions in the total area of some selected brain structures in the tMCAo group compared to Sham.

In the left hemisphere, significant reductions were seen in somatosensory cortex ($p < 0,0001$), motor cortex ($p < 0,01$) and visual cortex ($p < 0,01$) at L3. Regarding subcortical structures, significant reductions were seen in amygdaloid complex at L2 ($p < 0,01$) and L3 ($p < 0,001$) and in dorsal striatum at L1 ($p < 0,01$) on the left side. Although thalamus, hypothalamus and hippocampal formation showed visually slightly larger total areas in the Sham group on the left side and in the tMCAo group on the right side, there were no significant differences ($p > 0,05$).

Similar cortical and subcortical changes are also observed in the literature. A study done by Kessner et al. (2021) found that somatosensory disruption after ischemic stroke is common, supporting the significant total area reductions in the left side somatosensory cortex in the tMCAo group. Also, it found that both white matter (corpus callosum) and gray matter are correlates of acute somatosensory disruption after stroke, also adding to the concept of diaschisis, extending the impact of stroke beyond primary lesion (Kessner et al., 2021). However, it was seen that in tMCAo model mice there are changes in pyramidal neurons in the contralateral to lesion somatosensory cortex such as reduced dendritic complexity of apical dendritic arbors and reduced spine volume, suggesting reduced complexity of contralesional hemisphere (Merino-Serrais et al., 2023).

Interestingly, another study done by Mohajerani et al. (2011) showed that mini-targeted strokes in a somatosensory cortex caused rapid functional changes in the brain by redistributing sensory processing to the unaffected contralateral to lesion hemisphere. However, these changes were not mediated by corpus callosum but rather by thalamic connections and blocking thalamus before stroke induction would prevent the interhemispheric sensory redistribution. Therefore, this study concluded that acute ischemic stroke triggers thalamus-dependent reorganisation of sensory function beyond just loss of activity and that the brain can quickly compensate by activating subcortical circuits to maintain sensory function after focal damage (Mohajerani et al., 2011). This finding is important in the rehabilitation after stroke as stimulating subcortical circuits could help to regain lost functions.

For the thickness measurement, significant reductions ($p < 0,0001$) were seen in somatosensory and motor cortex on contralateral to lesion side at L2 in tMCAo group, yet, no significant differences were observed in visual cortex and hippocampal formation.

Supporting this finding, a study done in 2012 by Duering et al. using serial brain imaging, tractography and cortical thickness measurement showed that after infarcts there are significant

focal changes in cortical morphology (thinning) in those regions connected to the lesion (Duering et al., 2012). This may signal secondary neurodegeneration in the neurons with possible mechanisms of retrograde and anterograde degeneration, shrinkage and apoptosis of neuron cells (Siffrin et al., 2010). This phenomena of reduction in cortical and subcortical structures as a result of axonal degeneration after ischemic stroke was also supported in a study by Yu et al (2009) which showed that axonal disintegration and myelin degradation can lead to secondary degeneration of affected fiber tracts (Yu et al., 2009).

Importantly, the concept of diaschisis was supported in the contralateral to lesion motor cortex but in this study it was related to compensatory effect rather than classical “decreased” effect. In this study, a significant increase ($p < 0,0001$) in the total area of contralateral to lesion motor cortex in the tMCAo group was seen, indicating a compensatory outcome. However, other regions did not show significant changes suggesting that in this case, the motor cortex is the primary region affected by remote network influences and that the impact of diaschisis may be region-specific.

It has been seen that contralateral to lesion motor cortex has a supportive role in motor recovery after stroke. When the primary motor cortex or its cortico-spinal pathway is damaged, the contralesional to lesion primary motor cortex shows increased excitation which is linked to better motor outcomes. However, reducing this increased activity can worsen the performance of affected limb (Carr et al., 1993). A study done by Mima et al. (2001) using electroencephalogram-electromyogram (EEG-EMG) for wrist extensor and power grip muscles showed a reduction in EEG-EMG coherence on the affected side but increased coherence on the contralateral side suggesting that contralateral side preserved cortico-spinal connection (Mima et al., 2001). Yet, some studies, such as the one done by Werhahn et al. (2003) contradict the statement that the contralateral hemisphere takes over motor function. In this study, transcranial magnetic stimulation (TMS) was used on both ipsilateral and contralateral hemispheres. As a result, stimulation of the intact hemisphere did not show significant changes in motor activation of the paretic hand whereas stimulation of the lesioned hemisphere showed a delay in reaction time in the paretic hand, suggesting that recovered motor function is related to the affected hemisphere (Werhahn et al., 2003). In line with this, Calautti & Baron (2003) summarised that after stroke, recovery of motor function is related to both ipsilesional and contralesional motor cortex, suggesting an interplay between both regions.

Interestingly, in the tMCAo group there was also a significant increase seen in the total area of the right hemisphere at all Bregma levels. This observation also adds up to the diaschisis concept. It may indicate structural reorganisation in the contralesional to lesion hemisphere, possibly reflecting compensatory plasticity. A study done by Xing. et al (2016) on 32 left hemisphere stroke patients found a compensatory role of the right hemisphere after the stroke due to the increased grey matter

volume in the right temporoparietal cortex, mostly in supramarginal gyrus and posterior superior temporal gyrus. This change positively correlated with enhanced verbal working memory and pseudoword repetition, suggesting evidence for structural plasticity in the right hemisphere, contributing to language recovery after left hemisphere stroke (Xing et al., 2016). Moreover, another study also found similar results related to improved language outcomes due to the long-term plasticity of the right hemisphere which, on untraditional note, persisted years after the stroke. Hope et al. (2017) showed that there are structural changes in the right hemisphere, particularly hypertrophy in the anterior temporal lobe, that are associated with improved language function. However, they also showed that in the right precentral gyrus there is a decline in language ability, concluding that not all compensatory adaptations are positive (Hope et al., 2017).

These studies support the idea that structural increase in the area of the right hemisphere after left hemisphere stroke may be due to the compensatory neuroplasticity, where the right side tries to overcompensate by supporting the functions that were previously managed by the damaged left hemisphere.

Therefore, these findings are important in the context of recovery after ischemic stroke and are consistent with reports of compensatory plasticity or diaschisis, where the unaffected hemisphere attempts to support recovery but the ipsilateral to lesion side should not be dismissed. The most effective recovery process seems to be involving both hemispheres where the ipsilateral side remains essential for motor control whereas the contralesional side may support the recovery through neuroplasticity mechanisms.

Regarding the strengths and limitations of this study, one of the strengths was the use of the tMCAo mice model which is the most commonly used animal model in the study of ischemic stroke, mimicking the pathology in human ischemic stroke. On the other hand, animal models cannot fully represent the complexity of human stroke making results not 100% adaptable in human studies. Moreover, presented measurements may be affected by staining variability and tissue selection and a small sample size may prevent conclusive research evidence. In the future, a larger sample size may present more validated results and show more significant changes in selected brain regions.

Conclusions and recommendations

The present study investigated anatomical changes in cortical and subcortical structures using the tMCAo model in mice and founded that:

- There are significant reductions in the total area of key brain structures in the tMCAo group compared to Sham mainly on the ipsilateral to lesion side, specifically in somatosensory, motor and visual cortex with significant reductions in total area, supporting the idea that ischemic stroke results in severe structural damage in cortical regions.
- Subcortical structures such as the amygdaloid complex, corpus callosum and dorsal striatum also showed significant reductions in total area on the ipsilateral side to lesion, supporting the idea that stroke induces damage beyond primary cortical areas. Also, the observed thinning of cortical structures further highlights the impact of ischemic injury suggesting secondary neuronal degeneration.
- A significant increase in the total area of the right hemisphere and contralateral to lesion motor cortex suggests a compensatory effect, highlighting the concept of diaschisis or contralesional reorganisation and complex interplay between ipsilateral and contralateral to lesion hemispheres during recovery.
- While there were no statistically significant differences in the total area of thalamus, hypothalamus and hippocampal formation and in the thickness of visual cortex and hippocampal formation, a clear tendency of increased measurements in the tMCAo group on the contralateral to lesion side was observed potentially indicating that stroke has global effects on the whole-brain.

Although the research on diaschisis is still relatively new and mechanisms of plastic changes in brain areas distant from the lesion remain unclear, it attracts more scientific attention due to the advancements in neuroimaging, which allow to assess actual changes in the whole-brain connectome. Therefore, further studies could focus on examining structural alterations and contralesional plasticity, including changes in size and thickness of cortical and subcortical regions connected to the lesion. Additionally, research could investigate the compensatory effect of distant regions from the lesion and their contribution to functional recovery after stroke, supporting the development of new rehabilitation strategies that would target both hemispheres as they seem to be impacted by stroke.

Authors personal contribution

The author has contributed to the following work: identifying and selecting tissue samples; tissue mounting on slides and performing Nissl staining; using a microscope and camera to take pictures of stained tissue samples; identifying brain structures and tracing them with NeuroLucida software; extracting data with NeuroLucida NeuroExplorer; statistically analysing data with GraphPad Prism; making figures and tables.

Acknowledgments

I would like to sincerely thank my thesis supervisor Dr. Asta Kastanauskaitė for a practice opportunity and for her invaluable guidance, support and encouragement throughout this research. Also, a special thanks to my consultant Dr. Paula Merino-Serrais for her expert insights and collaboration on statistical analysis.

Funding

This work was supported by the following grants: Network of European Funding for Neuroscience Research (ERA-NET NEURON, PCI2018-092874), the Spanish Ministerio de Ciencia, Innovación y Universidades (grant IJCI-2016-27658 to P.M.S. and grant PGC2018-094307-B-I00 to J.D.), the Interdisciplinary Platform Cajal Blue Brain (CSIC, Spain), the Centro de Investigación Biomédica en Red sobre Enfermedades Neurodegenerativas (CIBERNED, CB06/05/0066, Spain) and the Deutsche Forschungsgemeinschaft (DFG, German Research Foundation) under Germany's Excellence Strategy within the framework of the Munich Cluster for Systems Neurology (EXC 2145 SyNergy – ID 390857198) to NP. *Conflict of interest statement.* The authors declare that they have no competing interest.

Anatominiai priešingo smegenų pusrutulio pakitimai išeminio insulto modelyje (MCAo)

Santrauka

Išeminis insultas tebėra vienas iš pagrindinių mirtingumo ir ilgalaikio neįgalumo priežasčių pasaulyje. Nors jo pirminė smegenų pažeidimo yra gerai ištirta, vis dar trūksta žinių apie anatominius pokyčius nutolusiuose, su pažeista sritimi susijusiuose regionuose, apibendrinančius reiškinių, žinomą kaip diaschizė. Šių pokyčių supratimas yra svarbus patologijos, gydymo ir reabilitacijos atvejais. Šio darbo tikslas buvo analizuoti ir palyginti anatominius pokyčius po insulto ipsilateralinėje ir kontralateralinėje pusrutulio žievėse ir požievės smegenų struktūrose, naudojant laikiną vidurinės smegenų arterijos okliuzijos (tMCAo) pelės modelį su pažeidimu kairėje smegenų pusėje. C57BL/6N patinai buvo suskirstyti į Sham (kontrolinę) ir tMCAo (eksperimentinę) grupes. Smegenų pjūviai buvo dažyti naudojant Nissl metodą ir analizuoti trijuose Bregma intervaluose. Pasirinktose smegenų srityse (pusrutuliuose, didžiojoje smegenų jungtyje, somatosorinėje, motorinėje ir regimojoje žievėse, migdolinio kūno komplekse, gumbure, pogumburyje, hipokampo darinyje ir nugariniame dryžuotame kūne) buvo matuojamas bendras plotas ir struktūros plotis naudojant NeuroLucida 360 programinę įrangą, o skirtumai buvo statistiškai analizuojami naudojant neparametrinį Mann-Whitney testą. Gauti rezultatai parodė reikšmingus pokyčius abiejose pusrutulio pusėse. Ipsilateralinėje insultui pusėje bendras plotas buvo sumažėjęs somatosensorinėje ir motorinėje žievėje, nugariniame dryžuotame kūne ir migdolinio kūno komplekse. Tačiau priešingoje, kontralateralinėje insultui pusėje, bendras plotas buvo padidėjęs pačio dešiniojo pusrutulio ir motorinės žievės. Šie rezultatai patvirtina anatomines reorganizacijos idėją ir palaiko diaschizės konceptą. Taip pat, jie prisideda prie gilesnio insulto patologijos supratimo, suteikia galimybių tikslinėms insulto reabilitacijos strategijoms bei suteikia gaires būsimiems ultrastruktūriniais tyrimams naudojant elektroninį mikroskopą.

Eglė Meškauskaitė

Master's thesis

**Anatomical alterations in the contralateral brain hemisphere in an ischemic stroke model
(tMCAo)**

Abstract

Ischemic stroke remains one of the leading causes of mortality and long-term disability worldwide. While its primary damage is well analysed, less is known about anatomical alterations in distant, connected brain regions in a phenomenon known as diaschisis and understanding of these alterations is essential in case of pathology, treatment and recovery. This study aimed to analyse and compare post-stroke anatomical changes in cortical and subcortical brain regions of the ipsilateral to lesion and contralateral to lesion hemispheres using a transient middle cerebral artery occlusion (tMCAo) mouse model which had induced lesion on left side. Male C57BL/6N mice were divided into Sham (control) and tMCAo (experimental) groups. Coronal brain sections were Nissl stained and analyzed across three Bregma intervals. Total area and cortical thickness were measured in selected brain regions (hemispheres, corpus callosum, somatosensory cortex, motor cortex, visual cortex, amygdaloid complex, thalamus, hypothalamus, hippocampal formation and dorsal striatum) using NeuroLucida 360 software and differences were statistically analysed using non-parametric Mann-Whitney test. Significant bilateral alterations were observed. On the ipsilateral to lesion side, total area was reduced in somatosensory and motor cortices, dorsal striatum and amygdaloid complex. In contrast, the contralateral to lesion side showed an increase in the total area of the right hemisphere and motor cortex. These findings validate the idea of anatomical reorganisation and support the diaschisis concept, contributing to a deeper understanding of stroke pathology and offering potential for targeted stroke recovery strategies as well as guidance for future ultrastructural studies using electron microscopy.

References

- Adams Jr, H.P., Bendixen, B.H., Kappelle, L.J., Biller, J., Love, B.B., Gordon, D.L. and Marsh 3rd, E.E., 1993. Classification of subtype of acute ischemic stroke. Definitions for use in a multicenter clinical trial. TOAST. Trial of Org 10172 in Acute Stroke Treatment. *stroke*, 24(1), pp.35-41.
- Alistair Lammie, G., 2000. Pathology of small vessel stroke. *British medical bulletin*, 56(2), pp.296-306.
- Balleine, B.W., Delgado, M.R. and Hikosaka, O., 2007. The role of the dorsal striatum in reward and decision-making. *Journal of Neuroscience*, 27(31), pp.8161-8165.
- Banerjee, C., Moon, Y.P., Paik, M.C., Rundek, T., Mora-McLaughlin, C., Vieira, J.R., Sacco, R.L. and Elkind, M.S., 2012. Duration of diabetes and risk of ischemic stroke: the Northern Manhattan Study. *Stroke*, 43(5), pp.1212-1217.
- Baron, J.C., Rougemont, D., Soussaline, F., Bustany, P., Crouzel, C., Bousser, M.G. and Comar, D., 1984. Local interrelationships of cerebral oxygen consumption and glucose utilization in normal subjects and in ischemic stroke patients: a positron tomography study. *Journal of Cerebral Blood Flow & Metabolism*, 4(2), pp.140-149.
- Boehme, A.K., Esenwa, C. and Elkind, M.S., 2017. Stroke risk factors, genetics, and prevention. *Circulation research*, 120(3), pp.472-495.
- Bonita, R., 1992. Epidemiology of stroke. *The Lancet*, 339(8789), pp.342-344.
- Buchan, A.M., Xue, D. and Slivka, A., 1992. A new model of temporary focal neocortical ischemia in the rat. *Stroke*, 23(2), pp.273-279.
- Butz, M., Steenbuck, I.D. and van Ooyen, A., 2014. Homeostatic structural plasticity can account for topology changes following deafferentation and focal stroke. *Frontiers in Neuroanatomy*, 8, p.115.
- Cadwell, C.R., Bhaduri, A., Mostajo-Radji, M.A., Keefe, M.G. and Nowakowski, T.J., 2019. Development and arealization of the cerebral cortex. *Neuron*, 103(6), pp.980-1004.
- Carmichael, S.T., 2005. Rodent models of focal stroke: size, mechanism, and purpose. *NeuroRx*, 2(3), pp.396-409.
- Carr, L.J., Harrison, L.M., Evans, A.L. and Stephens, J.A., 1993. Patterns of central motor reorganization in hemiplegic cerebral palsy. *Brain*, 116(5), pp.1223-1247.
- Chaturvedi, S. and Bhattacharya, P., 2014. Large artery atherosclerosis: carotid stenosis, vertebral artery disease, and intracranial atherosclerosis. *CONTINUUM: Lifelong Learning in Neurology*, 20(2), pp.323-334.
- Chauhan, G. and Debette, S., 2016. Genetic risk factors for ischemic and hemorrhagic stroke. *Current cardiology reports*, 18(12), p.124.

- Cheng, M.H., Lin, L.L., Liu, J.Y. and Liu, A.J., 2012. The outcomes of stroke induced by middle cerebral artery occlusion in different strains of mice. *CNS neuroscience & therapeutics*, 18(9), p.794.
- Chobanian, A.V., Bakris, G.L., Black, H.R., Cushman, W.C., Green, L.A., Izzo Jr, J.L., Jones, D.W., Materson, B.J., Oparil, S., Wright Jr, J.T. and Roccella, E.J., 2003. The seventh report of the joint national committee on prevention, detection, evaluation, and treatment of high blood pressure: the JNC 7 report. *Jama*, 289(19), pp.2560-2571.
- Cole, J.W., 2017. Large artery atherosclerotic occlusive disease. *CONTINUUM: Lifelong Learning in Neurology*, 23(1), pp.133-157.
- Cruz-Flores, S., Rabinstein, A., Biller, J., Elkind, M.S., Griffith, P., Gorelick, P.B., Howard, G., Leira, E.C., Morgenstern, L.B., Ovbiagele, B. and Peterson, E., 2011. Racial-ethnic disparities in stroke care: the American experience: a statement for healthcare professionals from the American Heart Association/American Stroke Association. *Stroke*, 42(7), pp.2091-2116.
- Darby, R.R., Horn, A., Cushman, F. and Fox, M.D., 2018. Lesion network localization of criminal behavior. *Proceedings of the National Academy of Sciences*, 115(3), pp.601-606.
- Di Carlo, A., 2009. Human and economic burden of stroke. *Age and ageing*, 38(1), pp.4-5.
- Dietrich, W.D., Ginsberg, M.D., Busto, R. and Watson, B.D., 1986. Photochemically induced cortical infarction in the rat. 1. Time course of hemodynamic consequences. *Journal of Cerebral Blood Flow & Metabolism*, 6(2), pp.184-194.
- Dirnagl, U. and Macleod, M.R., 2009. Stroke research at a road block: the streets from adversity should be paved with meta-analysis and good laboratory practice. *British journal of pharmacology*, 157(7), pp.1154-1156.
- Domercq, M., Sánchez-Gómez, M.V., Sherwin, C., Etxebarria, E., Fern, R. and Matute, C., 2007. System xc⁻ and glutamate transporter inhibition mediates microglial toxicity to oligodendrocytes. *The Journal of Immunology*, 178(10), pp.6549-6556.
- Domercq, M. and Matute, C., 2019. Excitotoxicity therapy for stroke patients still alive. *EBioMedicine*, 39, pp.3-4.
- Drake, R.L., Vogl, A.W., and Mitchell, A.W.M. (2023) 'Neuroanatomy', in Gray's Anatomy for Students. 5th edn. St. Louis, MO: Elsevier, pp. e1–e72.
- Dronkers, N.F., Plaisant, O., Iba-Zizen, M.T. and Cabanis, E.A., 2007. Paul Broca's historic cases: high resolution MR imaging of the brains of Leborgne and Lelong. *Brain*, 130(5), pp.1432-1441
- Duering, M., Righart, R., Csanadi, E., Jouvent, E., Hervé, D., Chabriat, H. and Dichgans, M., 2012. Incident subcortical infarcts induce focal thinning in connected cortical regions. *Neurology*, 79(20), pp.2025-2028.

- Duverger, D. and MacKenzie, E.T., 1988. The quantification of cerebral infarction following focal ischemia in the rat: influence of strain, arterial pressure, blood glucose concentration, and age. *Journal of Cerebral Blood Flow & Metabolism*, 8(4), pp.449-461.
- Feske, S.K., 2021. Ischemic stroke. *The American journal of medicine*, 134(12), pp.1457-1464.
- Fluri, F., Schuhmann, M.K. and Kleinschnitz, C., 2015. Animal models of ischemic stroke and their application in clinical research. *Drug design, development and therapy*, pp.3445-3454.
- Fuxe, K., Bjelke, B., Andbjør, B., Grahn, H., Rimondini, R. and Agnati, L.F., 1997. Endothelin-1 induced lesions of the frontoparietal cortex of the rat. A possible model of focal cortical ischemia. *Neuroreport*, 8(11), pp.2623-2629.
- GBD 2021 Stroke Risk Factor Collaborators, 2024. *Global, regional, and national burden of stroke and its risk factors, 1990–2021: a systematic analysis for the Global Burden of Disease Study 2021*. The Lancet Neurology.
- Gerriets, T., Li, F., Silva, M.D., Meng, X., Brevard, M., Sotak, C.H. and Fisher, M., 2003. The macrosphere model: evaluation of a new stroke model for permanent middle cerebral artery occlusion in rats. *Journal of neuroscience methods*, 122(2), pp.201-211.
- Hacke, W., Kaste, M., Bluhmki, E., Brozman, M., Dávalos, A., Guidetti, D., Larrue, V., Lees, K.R., Medeghri, Z., Machnig, T. and Schneider, D., 2008. Thrombolysis with alteplase 3 to 4.5 hours after acute ischemic stroke. *New England journal of medicine*, 359(13), pp.1317-1329.
- Hankey, G.J. and Blacker, D.J., 2015. Is it a stroke?. *Bmj*, 350
- Hartwigsen, G., Bengio, Y. and Bzdok, D., 2021. How does hemispheric specialization contribute to human-defining cognition?. *Neuron*, 109(13), pp.2075-2090.
- Hayakawa, K., Mishima, K., Nozako, M., Hazekawa, M., Mishima, S., Fujioka, M., Orito, K., Egashira, N., Iwasaki, K. and Fujiwara, M., 2008. Delayed treatment with minocycline ameliorates neurologic impairment through activated microglia expressing a high-mobility group box1–inhibiting mechanism. *Stroke*, 39(3), pp.951-958.
- Hilkens, N.A., Casolla, B., Leung, T.W. and de Leeuw, F.E., 2024. The Stroke. *Lancet*, 403(10446), pp.2820-2836.
- Hope, T.M., Leff, A.P., Prejawa, S., Bruce, R., Haigh, Z., Lim, L., Ramsden, S., Oberhuber, M., Ludersdorfer, P., Crinion, J. and Seghier, M.L., 2017. Right hemisphere structural adaptation and changing language skills years after left hemisphere stroke. *Brain*, 140(6), pp.1718-1728.
- Hossmann, K.A., 2012. The two pathophysiologies of focal brain ischemia: implications for translational stroke research. *Journal of Cerebral Blood Flow & Metabolism*, 32(7), pp.1310-1316
- Howells, D.W., Porritt, M.J., Rewell, S.S., O'collins, V., Sena, E.S., Van Der Worp, H.B., Traystman, R.J. and Macleod, M.R., 2010. Different strokes for different folks: the rich diversity

- of animal models of focal cerebral ischemia. *Journal of Cerebral Blood Flow & Metabolism*, 30(8), pp.1412-1431.
- Hughes, P.M., Anthony, D.C., Ruddin, M., Botham, M.S., Rankine, E.L., Sablone, M., Baumann, D., Mir, A.K. and Perry, V.H., 2003. Focal lesions in the rat central nervous system induced by endothelin-1. *Journal of Neuropathology & Experimental Neurology*, 62(12), pp.1276-1286.
- Husain, J. and Juurlink, B.H., 1995. Oligodendroglial precursor cell susceptibility to hypoxia is related to poor ability to cope with reactive oxygen species. *Brain research*, 698(1-2), pp.86-94.
- Hwang, J.Y., Gertner, M., Pontarelli, F., Court-Vazquez, B., Bennett, M.V.L., Ofengeim, D. and Zukin, R.S., 2017. Global ischemia induces lysosomal-mediated degradation of mTOR and activation of autophagy in hippocampal neurons destined to die. *Cell Death & Differentiation*, 24(2), pp.317-329.
- Iaccarino, G., Ciccarelli, M., Sorriento, D., Galasso, G., Campanile, A., Santulli, G., Cipolletta, E., Cerullo, V., Cimini, V., Altobelli, G.G. and Piscione, F., 2005. Ischemic neoangiogenesis enhanced by β 2-adrenergic receptor overexpression: a novel role for the endothelial adrenergic system. *Circulation research*, 97(11), pp.1182-1189.
- Iadecola, C., Park, L. and Capone, C., 2009. Threats to the mind: aging, amyloid, and hypertension. *Stroke*, 40(3_suppl_1), pp.S40-S44.
- John Stirling (2000) *Cortical Functions*. London: Routledge. Available at: <https://research.ebsco.com/linkprocessor/plink?id=6670fe48-6105-38aa-820e-47e66d0774c5> (Accessed: 18 April 2025).
- Keil, K. and Kaszniak, A.W., 2002. Examining executive function in individuals with brain injury: A review. *Aphasiology*, 16(3), pp.305-335.
- KEMPINSKY, W.H., 1958. Experimental study of distant effects of acute focal brain injury: a study of diaschisis. *AMA Archives of Neurology & Psychiatry*, 79(4), pp.376-389.
- Kessner, S.S., Schlemm, E., Cheng, B., Bingel, U., Fiehler, J., Gerloff, C. and Thomalla, G., 2019. Somatosensory deficits after ischemic stroke: time course and association with infarct location. *Stroke*, 50(5), pp.1116-1123.
- Kessner, S.S., Schlemm, E., Gerloff, C., Thomalla, G. and Cheng, B., 2021. Grey and white matter network disruption is associated with sensory deficits after stroke. *NeuroImage: Clinical*, 31, p.102698.
- Kim, J., Thayabaranathan, T., Donnan, G.A., Howard, G., Howard, V.J., Rothwell, P.M., Feigin, V., Norrving, B., Owolabi, M., Pandian, J. and Liu, L., 2020. Global stroke statistics 2019. *International Journal of Stroke*, 15(8), pp.819-838.
- Kim, J.S., 1992. Pure sensory stroke. Clinical-radiological correlates of 21 cases. *Stroke*, 23(7), pp.983-987.

- Kleindorfer, D., Panagos, P., Pancioli, A., Khoury, J., Kissela, B., Woo, D., Schneider, A., Alwell, K., Jauch, E., Miller, R. and Moomaw, C., 2005. Incidence and short-term prognosis of transient ischemic attack in a population-based study. *Stroke*, 36(4), pp.720-723.
- Kuriakose, D. and Xiao, Z., 2020. Pathophysiology and treatment of stroke: present status and future perspectives. *International journal of molecular sciences*, 21(20), p.7609.
- Lang, C.E., Bland, M.D., Bailey, R.R., Schaefer, S.Y. and Birkenmeier, R.L., 2013. Assessment of upper extremity impairment, function, and activity after stroke: foundations for clinical decision making. *Journal of Hand Therapy*, 26(2), pp.104-115.
- Laucevičius, A., Rinkūnienė, E., Petrulionienė, Ž., Ryliškytė, L., Jucevičienė, A., Purnaitė, R., Badarienė, J., Navickas, R., Mikolaitytė, J., Gargalskaitė, U. and Dženkevičiūtė, V., 2020. Trends in cardiovascular risk factor prevalence among Lithuanian middle-aged adults between 2009 and 2018. *Atherosclerosis*, 299, pp.9-14.
- Lee, J.S., Hong, J.M., Moon, G.J., Lee, P.H., Ahn, Y.H. and Bang, O.Y., 2010. A long-term follow-up study of intravenous autologous mesenchymal stem cell transplantation in patients with ischemic stroke. *Stem cells*, 28(6), pp.1099-1106.
- Lee, K.B., Lim, S.H., Kim, K.H., Kim, K.J., Kim, Y.R., Chang, W.N., Yeom, J.W., Kim, Y.D. and Hwang, B.Y., 2015. Six-month functional recovery of stroke patients: a multi-time-point study. *International journal of rehabilitation research*, 38(2), pp.173-180.
- Leśniak, M., Bak, T., Czepiel, W., Seniów, J. and Członkowska, A., 2008. Frequency and prognostic value of cognitive disorders in stroke patients. *Dementia and geriatric cognitive disorders*, 26(4), pp.356-363.
- Li, L., Simoni, M., Küker, W., Schulz, U.G., Christie, S., Wilcock, G.K. and Rothwell, P.M., 2013.
- Li, W.A., Geng, X. and Ding, Y., 2017. Stroke is a global epidemic: new developments in clinical and translational cerebrovascular diseases research. *Neurological research*, 39(6), pp.475-476.
- Liebesskind, D.S., 2003. Collateral circulation. *Stroke*, 34(9), pp.2279-2284.
- Lim, C. and Alexander, M.P., 2009. Stroke and episodic memory disorders. *Neuropsychologia*, 47(14), pp.3045-3058.
- Lin, H.J., Wolf, P.A., Kelly-Hayes, M., Beiser, A.S., Kase, C.S., Benjamin, E.J. and D'Agostino, R.B., 1996. Stroke severity in atrial fibrillation: the Framingham Study. *Stroke*, 27(10), pp.1760-1764.
- Lipton, P., 1999. Ischemic cell death in brain neurons. *Physiological reviews*.
- Liu, S., Zhen, G., Meloni, B.P., Campbell, K. and Winn, H.R., 2009. Rodent stroke model guidelines for preclinical stroke trials. *Journal of experimental stroke & translational medicine*, 2(2), p.2.

- Maeda, K., Hata, R. and Hossmann, K.A., 1999. Regional metabolic disturbances and cerebrovascular anatomy after permanent middle cerebral artery occlusion in C57black/6 and SV129 mice. *Neurobiology of disease*, 6(2), pp.101-108.
- Maitrias, P., Metzinger-Le Meuth, V., Nader, J., Reix, T., Caus, T. and Metzinger, L., 2017. The involvement of miRNA in carotid-related stroke. *Arteriosclerosis, Thrombosis, and Vascular Biology*, 37(9), pp.1608-1617.
- Mashour, G.A. and Pryor, K.O., 2015. Consciousness, memory, and anesthesia. *Miller's anesthesia, 9th Edn. Philadelphia: Elsevier*, pp.250-266.
- McAuley, M.A., 1995. Rodent models of focal ischemia. *Cerebrovascular and brain metabolism reviews*, 7(2), pp.153-180.
- McColl, B.W., Carswell, H.V., McCulloch, J. and Horsburgh, K., 2004. Extension of cerebral hypoperfusion and ischaemic pathology beyond MCA territory after intraluminal filament occlusion in C57Bl/6J mice. *Brain research*, 997(1), pp.15-23.
- Merino-Serrais, P., Plaza-Alonso, S., Hellal, F., Valero-Freitag, S., Kastanauskaite, A., Muñoz, A., Plesnila, N. and DeFelipe, J., 2023. Microanatomical study of pyramidal neurons in the contralesional somatosensory cortex after experimental ischemic stroke. *Cerebral Cortex*, 33(4), pp.1074-1089.
- Meyer, S., Kessner, S.S., Cheng, B., Bönstrup, M., Schulz, R., Hummel, F.C., De Bruyn, N., Peeters, A., Van Pesch, V., Duprez, T. and Sunaert, S., 2016. Voxel-based lesion-symptom mapping of stroke lesions underlying somatosensory deficits. *NeuroImage: Clinical*, 10, pp.257-266.
- Mima, T., Toma, K., Koshy, B. and Hallett, M., 2001. Coherence between cortical and muscular activities after subcortical stroke. *Stroke*, 32(11), pp.2597-2601.
- Mohajerani, M.H., Aminoltejari, K. and Murphy, T.H., 2011. Targeted mini-strokes produce changes in interhemispheric sensory signal processing that are indicative of disinhibition within minutes. *Proceedings of the National Academy of Sciences*, 108(22), pp.E183-E191.
- Nakagomi, S., Kiryu-Seo, S. and Kiyama, H., 2000. Endothelin-converting enzymes and endothelin receptor B messenger RNAs are expressed in different neural cell species and these messenger RNAs are coordinately induced in neurons and astrocytes respectively following nerve injury. *Neuroscience*, 101(2), pp.441-449.
- Niessen, F., Hilger, T., Hoehn, M. and Hossmann, K.A., 2003. Differences in clot preparation determine outcome of recombinant tissue plasminogen activator treatment in experimental thromboembolic stroke. *Stroke*, 34(8), pp.2019-2024.
- Overgaard, K., 1994. Thrombolytic therapy in experimental embolic stroke. *Cerebrovascular and brain metabolism reviews*, 6(3), pp.257-286.

- Parnavelas, J.G., 2002. The origin of cortical neurons. *Brazilian journal of medical and biological research*, 35, pp.1423-1429.
- Pawluk, H., Kołodziejaska, R., Grzešek, G., Woźniak, A., Kozakiewicz, M., Kosinska, A., Pawluk, M., Grzechowiak, E., Wojtasik, J. and Kozera, G., 2022. Increased oxidative stress markers in acute ischemic stroke patients treated with thrombolytics. *International Journal of Molecular Sciences*, 23(24), p.15625.
- Paxinos, G. and Franklin, K.B., 2019. *Paxinos and Franklin's the mouse brain in stereotaxic coordinates*. Academic press.
- Peng, L., Hu, G., Yao, Q., Wu, J., He, Z., Law, B.Y.K., Hu, G., Zhou, X., Du, J., Wu, A. and Yu, L., 2022. Microglia autophagy in ischemic stroke: A double-edged sword. *Frontiers in immunology*, 13, p.1013311.
- Population-based case–control study of white matter changes on brain imaging in transient ischemic attack and ischemic stroke. *Stroke*, 44(11), pp.3063-3070.
- Power, C., Henry, S., Del Bigio, M.R., Larsen, P.H., Corbett, D., Imai, Y., Yong, V.W. and Peeling, J., 2003. Intracerebral hemorrhage induces macrophage activation and matrix metalloproteinases. *Annals of neurology*, 53(6), pp.731-742.
- Powers, W.J., Rabinstein, A.A., Ackerson, T., Adeoye, O.M., Bambakidis, N.C., Becker, K., Biller, J., Brown, M., Demaerschalk, B.M., Hoh, B. and Jauch, E.C., 2018. 2018 guidelines for the early management of patients with acute ischemic stroke: a guideline for healthcare professionals from the American Heart Association/American Stroke Association. *stroke*, 49(3), pp.e46-e99.
- Preusser, S., Thiel, S.D., Rook, C., Roggenhofer, E., Kosatschek, A., Draganski, B., Blankenburg, F., Driver, J., Villringer, A. and Pleger, B., 2015. The perception of touch and the ventral somatosensory pathway. *Brain*, 138(3), pp.540-548.
- Provenzale, J.M., Jahan, R., Naidich, T.P. and Fox, A.J., 2003. Assessment of the patient with hyperacute stroke: imaging and therapy. *Radiology*, 229(2), pp.347-359.
- Rabinstein, A.A., 2017. Treatment of acute ischemic stroke. *CONTINUUM: lifelong learning in neurology*, 23(1), pp.62-81.
- Raffin, E. and Hummel, F.C., 2018. Restoring motor functions after stroke: multiple approaches and opportunities. *The Neuroscientist*, 24(4), pp.400-416.
- Raichle, M.E., Larson, K.B., Phelps, M.E., Grubb Jr, R.L., Welch, M.J. and Ter-Pogossian, M.M., 1975. In vivo measurement of brain glucose transport and metabolism employing glucose--11C. *American Journal of Physiology-Legacy Content*, 228(6), pp.1936-1948.
- Rannikmäe, K., Woodfield, R., Anderson, C.S., Charidimou, A., Chiewvit, P., Greenberg, S.M., Jeng, J.S., Meretoja, A., Palm, F., Putaala, J. and Rinkel, G.J., 2016. Reliability of intracerebral

- hemorrhage classification systems: a systematic review. *International Journal of Stroke*, 11(6), pp.626-636.
- Regenhardt, R.W., Das, A.S., Lo, E.H. and Caplan, L.R., 2018. Advances in understanding the pathophysiology of lacunar stroke: a review. *JAMA neurology*, 75(10), pp.1273-1281.
- Reggia, J.A., 2004. Neurocomputational models of the remote effects of focal brain damage. *Medical engineering & physics*, 26(9), pp.711-722.
- Reid, E., Graham, D., Lopez-Gonzalez, M.R., Holmes, W.M., Macrae, I.M. and McCabe, C., 2012. Penumbra detection using PWI/DWI mismatch MRI in a rat stroke model with and without comorbidity: comparison of methods. *Journal of Cerebral Blood Flow & Metabolism*, 32(9), pp.1765-1777.
- Robinson, M.J., Macrae, I.M., Todd, M., Reid, J.L. and McCulloch, J., 1990. Reduction of local cerebral blood flow to pathological levels by endothelin-1 applied to the middle cerebral artery in the rat. *Neuroscience letters*, 118(2), pp.269-272.
- Rogers, L.J., 2021. Brain lateralization and cognitive capacity. *Animals*, 11(7), p.1996.
- Rolls, E.T., 2016. *Cerebral cortex: principles of operation*. Oxford University Press.
- Rose, C.R., Ziemens, D. and Verkhratsky, A., 2020. On the special role of NCX in astrocytes: Translating Na⁺-transients into intracellular Ca²⁺ signals. *Cell Calcium*, 86, p.102154.
- Russell, W.M.S., Burch, R.L. and Hume, C.W., 1959. *The principles of humane experimental technique* (Vol. 238, pp. 1-229). London: Methuen.
- Sacco, R.L., Kasner, S.E., Broderick, J.P., Caplan, L.R., Connors, J.J., Culebras, A., Elkind, M.S., George, M.G., Hamdan, A.D., Higashida, R.T. and Hoh, B.L., 2013. An updated definition of stroke for the 21st century: a statement for healthcare professionals from the American Heart Association/American Stroke Association. *Stroke*, 44(7), pp.2064-2089.
- Sachdev, P.S., Brodaty, H., Valenzuela, M.J., Lorentz, L. and Koschera, A., 2004. Progression of cognitive impairment in stroke patients. *Neurology*, 63(9), pp.1618-1623.
- Sah, P., Faber, E.L., Lopez de Armentia, M. and Power, J.M.J.P.R., 2003. The amygdaloid complex: anatomy and physiology. *Physiological reviews*, 83(3), pp.803-834.
- Salaudeen, M.A., Bello, N., Danraka, R.N. and Ammani, M.L., 2024. Understanding the pathophysiology of ischemic stroke: the basis of current therapies and opportunity for new ones. *Biomolecules*, 14(3), p.305.
- Saper, C.B. and Lowell, B.B., 2014. The hypothalamus. *Current Biology*, 24(23), pp.R1111-R1116.
- Schröder, H., Moser, N. and Huggenberger, S., 2020. *Neuroanatomy of the Mouse: An Introduction*. Cham: Springer Nature, pp. 59–61, 242–314.

- Shaheryar, Z.A., Khan, M.A., Adnan, C.S., Zaidi, A.A., Hänggi, D. and Muhammad, S., 2021. Neuroinflammatory triangle presenting novel pharmacological targets for ischemic brain injury. *Frontiers in immunology*, 12, p.748663.
- Sharkey, J., 1993. Perivascular microapplication of endothelin-1: a new model of focal cerebral ischaemia in the rat. *Journal of Cerebral Blood Flow & Metabolism*, 13(5), pp.865-871.
- Siffrin, V., Vogt, J., Radbruch, H., Nitsch, R. and Zipp, F., 2010. Multiple sclerosis—candidate mechanisms underlying CNS atrophy. *Trends in neurosciences*, 33(4), pp.202-210.
- Soto-Cámara, R., González-Bernal, J.J., González-Santos, J., Aguilar-Parra, J.M., Trigueros, R. and López-Liria, R., 2020. Knowledge on signs and risk factors in stroke patients. *Journal of clinical medicine*, 9(8), p.2557.
- Standring, S., 2021. *Cerebral hemispheres*. In: S. Standring, ed., *Gray's Anatomy: The Anatomical Basis of Clinical Practice*. 42nd ed. London: Elsevier, pp.512–539.e3.
- Stansbury, J.P., Jia, H., Williams, L.S., Vogel, W.B. and Duncan, P.W., 2005. Ethnic disparities in stroke: epidemiology, acute care, and postacute outcomes. *Stroke*, 36(2), pp.374-386.
- Stevens, E., Emmett, E., Wang, Y., McKevitt, C. and Wolfe, C., 2017. The burden of stroke in Europe.
- Sullivan, J.E. and Hedman, L.D., 2008. Sensory dysfunction following stroke: incidence, significance, examination, and intervention. *Topics in stroke rehabilitation*, 15(3), pp.200-217.
- Tamura, A., Graham, D.I., McCulloch, J. and Teasdale, G.M., 1981. Focal cerebral ischaemia in the rat: 1. Description of technique and early neuropathological consequences following middle cerebral artery occlusion. *Journal of Cerebral Blood Flow & Metabolism*, 1(1), pp.53-60.
- Ter Telgte, A., Van Leijssen, E.M., Wiegertjes, K., Klijn, C.J., Tuladhar, A.M. and de Leeuw, F.E., 2018. Cerebral small vessel disease: from a focal to a global perspective. *Nature Reviews Neurology*, 14(7), pp.387-398.
- Tikka, T.M. and Koistinaho, J.E., 2001. Minocycline provides neuroprotection against N-methyl-D-aspartate neurotoxicity by inhibiting microglia. *The Journal of Immunology*, 166(12), pp.7527-7533.
- Treadwell, S.D. and Thanvi, B., 2010. Malignant middle cerebral artery (MCA) infarction: pathophysiology, diagnosis and management. *Postgraduate medical journal*, 86(1014), pp.235-242.
- Tuo, Q.Z., Zhang, S.T. and Lei, P., 2022. Mechanisms of neuronal cell death in ischemic stroke and their therapeutic implications. *Medicinal research reviews*, 42(1), pp.259-305.
- Türeyen, K., Vemuganti, R., Sailor, K.A. and Dempsey, R.J., 2005. Ideal suture diameter is critical for consistent middle cerebral artery occlusion in mice. *Operative Neurosurgery*, 56(1), pp.196-200.

- U.S. Food and Drug Administration (2025) 'FDA Roundup: March 4, 2025'. Available at: <https://www.fda.gov/news-events/press-announcements/fda-roundup-march-4-2025> (Accessed: 28 April 2025).
- Uesugi, M., Kasuya, Y., Hayashi, K. and Goto, K., 1998. SB209670, a potent endothelin receptor antagonist, prevents or delays axonal degeneration after spinal cord injury. *Brain research*, 786(1-2), pp.235-239.
- Vanderah, T.W. and Gould, D.J., 2022. *Cerebral cortex*. In: T.W. Vanderah and D.J. Gould, eds. *Nolte's The Human Brain: An Introduction to its Functional Anatomy*. 8th ed. Philadelphia: Elsevier, pp.513–545.
- von Monakow, C., 1914. *Die Lokalisation im Grosshirn und der Abbau der Funktion durch kortikale Herde*. JF Bergmann.
- Wang, C.X., Todd, K.G., Yang, Y., Gordon, T. and Shuaib, A., 2001. Patency of cerebral microvessels after focal embolic stroke in the rat. *Journal of Cerebral Blood Flow & Metabolism*, 21(4), pp.413-421.
- Warlow, C.P., Van Gijn, J., Dennis, M.S., Wardlaw, J.M., Bamford, J.M., Hankey, G.J., Sandercock, P.A., Rinkel, G., Langhorne, P., Sudlow, C. and Rothwell, P., 2011. *Stroke: practical management*. John Wiley & Sons.
- Watson, B.D., Dietrich, W.D., Busto, R., Wachtel, M.S. and Ginsberg, M.D., 1985. Induction of reproducible brain infarction by photochemically initiated thrombosis. *Annals of Neurology: Official Journal of the American Neurological Association and the Child Neurology Society*, 17(5), pp.497-504.
- Werhahn, K.J., Conforto, A.B., Kadom, N., Hallett, M. and Cohen, L.G., 2003. Contribution of the ipsilateral motor cortex to recovery after chronic stroke. *Annals of Neurology: Official Journal of the American Neurological Association and the Child Neurology Society*, 54(4), pp.464-472.
- Woodruff, T.M., Thundyil, J., Tang, S.C., Sobey, C.G., Taylor, S.M. and Arumugam, T.V., 2011. Pathophysiology, treatment, and animal and cellular models of human ischemic stroke. *Molecular neurodegeneration*, 6, pp.1-19.
- Worden, A.N., 1947. *The UFAW handbook on the care and management of laboratory animals; with an appendix on statistical analysis*.
- World Health Organization, 2024. *Stroke, cerebrovascular accident*. World Health Organization. Available at: <https://www.who.int/data/gho/indicator-metadata-registry/imr-details/158> [Accessed 26 Apr. 2025].
- Writing Group Members, Roger, V.L., Go, A.S., Lloyd-Jones, D.M., Benjamin, E.J., Berry, J.D., Borden, W.B., Bravata, D.M., Dai, S., Ford, E.S. and Fox, C.S., 2012. Executive summary: heart

- disease and stroke statistics—2012 update: a report from the American Heart Association. *Circulation*, 125(1), pp.188-197.
- Xing, S., Lacey, E.H., Skipper-Kallal, L.M., Jiang, X., Harris-Love, M.L., Zeng, J. and Turkeltaub, P.E., 2016. Right hemisphere grey matter structure and language outcomes in chronic left hemisphere stroke. *Brain*, 139(1), pp.227-241.
- Xu, W., Jin, W., Zhang, X., Chen, J. and Ren, C., 2017. Remote limb preconditioning generates a neuroprotective effect by modulating the extrinsic apoptotic pathway and TRAIL-receptors expression. *Cellular and molecular neurobiology*, 37, pp.169-182.
- Yanagisawa, M., Kurihara, H., Kimura, S., Goto, K. and Masaki, T., 1988. A novel peptide vasoconstrictor, endothelin, is produced by vascular endothelium and modulates smooth muscle Ca²⁺ channels. *Journal of hypertension*, 6(4), pp.S188-191.
- Yiin, G.S., Howard, D.P., Paul, N.L., Li, L., Luengo-Fernandez, R., Bull, L.M., Welch, S.J., Gutnikov, S.A., Mehta, Z. and Rothwell, P.M., 2014. Age-specific incidence, outcome, cost, and projected future burden of atrial fibrillation-related embolic vascular events: a population-based study. *Circulation*, 130(15), pp.1236-1244.
- Yu, C., Zhu, C., Zhang, Y., Chen, H., Qin, W., Wang, M. and Li, K., 2009. A longitudinal diffusion tensor imaging study on Wallerian degeneration of corticospinal tract after motor pathway stroke. *Neuroimage*, 47(2), pp.451-458.
- Zarow, G., Karibe, H., States, B., Graham, S. and Weinstein, P., 1997. Endovascular suture occlusion of the middle cerebral artery in rats: effect of suture insertion distance on cerebral blood flow, infarct distribution and infarct volume. *Neurological research*, 19(4), pp.409-416.
- Zhuang, J., Ng, L., Williams, D., Valley, M., Li, Y., Garrett, M. and Waters, J., 2017. An extended retinotopic map of mouse cortex. *elife*, 6, p.e18372.